

THE ROLE OF XIN IN
SKELETAL MUSCLE REGENERATION

THE ROLE OF XIN IN SKELETAL MUSCLE REGENERATION

By

ALIYAH A. NISSAR, B.Sc.F.S

A Thesis Submitted to the School of Graduate Studies in Partial Fulfillment of the
Requirements for the Degree Master of Science

McMaster University© Copyright by Aliyah A. Nissar, December 2012

McMaster University MASTER OF SCIENCE (2012) Hamilton, Ontario (Medical Sciences)

TITLE: The role of Xin in skeletal muscle regeneration.

AUTHOR: Aliyah A. Nissar, B.Sc.F.S (Trent University)

SUPERVISOR: Professor Thomas J. Hawke

NUMBER OF PAGES: xii, 120

ABSTRACT

Adult skeletal muscle has the remarkable capacity of regenerating in response to stressors, such as overuse, injury, or myopathic conditions. A fundamental contributor to the regenerative process is satellite cells, which are the primary stem cells of skeletal muscle. Although the basic characteristics of these stem cells have been defined, the mechanistic factors regulating their function are still being determined. Uncovering such factors will greatly improve satellite cell therapeutic potential, especially for patients suffering from myopathic diseases.

The protein Xin was previously identified as being highly upregulated in damaged skeletal muscle, where it is otherwise observed at negligible levels. This lends to the idea that this striated muscle-specific cytoskeletal protein plays a role in the regenerative process. It was also shown that Xin is localized to the satellite cell population, although its purpose there has not been elucidated.

Therefore the overall goal of this study was to determine the role of Xin during skeletal muscle regeneration and within its resident stem cell population. This was approached using Xin knockdown (Xin shRNA) and knockout (Xin^{-/-} mice) models, whereby any deficits or changes in the regenerative process can be attributed to the lack/absence of Xin. The results of the following studies reveal that when Xin expression is reduced or absent, muscle regeneration is impaired, satellite cell activation is altered, and muscle fiber morphology moves towards a myopathic state.

Furthermore, since Xin has been shown to be upregulated during regeneration, it was interesting to study the expression of Xin in human myopathic muscle which is in a constant state of regeneration. In doing so, it was observed that the expression of Xin correlates with degree of damage in myopathic muscle, regardless of disease diagnosis. Therefore, these data have improved our understanding of muscle regeneration, satellite cell function, and suggest a clinical marker for defining muscle damage severity.

ACKNOWLEDGEMENTS:

This work is the result of the contribution of many individuals, to whom I am indebted to. First and foremost, Dr. Thomas Hawke who designed this project: thank you for being an excellent mentor, providing me with countless opportunities to help me grow as a scientist, and most of all, believing in me. Words cannot describe how much I appreciate your guidance and understanding, especially during the final lap. To Dr. Tarnopolsky and Dr. Parise, thank you for your invaluable input towards this research. Your expertise is much appreciated, as I couldn't have asked for more knowledgeable committee members. To our collaborators in Germany, Dr. Peter van der Ven and Dr. Dieter Fürst, thank you for your support and welcoming us into your lab. Special thanks to Sibylle Molt for taking the time to introduce us to the lab and Bonn. We would have been lost (literally) without you.

I am especially thankful to my labmates, both past and present, for their support and willingness to help, I couldn't have asked for a better bunch to work with. Particularly, Matthew Krause, Karin Trajcevski, and Jasmin Moradi for passing on your expertise to me, and Dhuha Al-Sajee for your words of wisdom. Donna D'Souza, thank you for all the memories we created in Europe, and for taking 'the jump' with me.

To my parents, Rabeka Nissar and Azeez Yussuf, thank you for giving me the freedom to make my own decisions and supporting every one of them. To my Dad, Khaleel Nissar, it is from you I inherited the determination to take the road less travelled (may you rest in eternal peace). To the rest of my family, especially Mohomed, Ryhan, Imtiaz & Sherene Nissar, Mohamed & Azeeman Ayub, and the 'Ayub clan', thank you all for instilling in

me the importance of education. I will continue to strive to make you all proud. Finally to my sisters, Jenessa Bhimsingh, Rashni Rajagopal, Rebecca Reginorld, and Sharnjit Moondi, thank you for being my sanity every step of the way. This work is dedicated to my extensive network of family and friends. I am so grateful for your love and encouragement over the past few years and as I continue on in my career.

PREFACE

This thesis is a “sandwich” style thesis. Chapter 1 constitutes the general introduction. Chapters 2, 3, 4 have been published or will be submitted for publication as peer-reviewed research papers. A preface of each chapter describes the details of the submitted articles, as well as my contribution to the multiple-authored work. Chapter 5 consists of an overall discussion and conclusion of the studies.

All chapters have been reproduced with permission of all co-authors. Irrevocable, non-exclusive licenses have been granted to McMaster University and to the National Library of Canada from all publishers.

TABLE OF CONTENTS

ABSTRACT	iii
ACKNOWLEDGEMENT	v
PREFACE	vii
TABLE OF CONTENTS	viii
LIST OF TABLES AND FIGURES	x
LIST OF ABBREVIATIONS	xi
CHAPTER 1. General introduction	
1.1. Introduction.....	1
1.2. Skeletal muscle repair.....	2
1.3. Satellite cells	6
1.4. Xin.....	8
1.5. Regeneration and myopathy	10
1.6. Conclusions	12
References.....	13
CHAPTER 2. Skeletal muscle regeneration is delayed by reduction in Xin expression: consequence of impaired satellite cell activation?	
Preface.....	20
Abstract.....	23
2.1. Introduction.....	24
2.2. Methods	26
2.3. Results.....	34
2.4. Discussion.....	40
2.5. Figures.....	44
References.....	50
CHAPTER 3. Skeletal muscle and satellite cell characterization of Xin-deficient mice	
Preface.....	54
Abstract.....	57
3.1. Introduction.....	58
3.2. Methods.....	60
3.3. Results.....	68
3.4. Discussion.....	73
3.5. Figures.....	76
References.....	82

CHAPTER 4. Xin: A marker of skeletal muscle damage severity in myopathic patients

Preface.....	85
Abstract.....	88
4.1. Introduction.....	90
4.2. Methods.....	92
4.3. Results.....	96
4.4. Discussion.....	99
4.5. Tables and Figures.....	103
References.....	111
CHAPTER 5. General discussion and conclusions.....	115
References.....	119

LIST OF TABLES AND FIGURES

CHAPTER 2

Figure 2.1 Immunohistochemical expression of Xin during skeletal muscle regeneration.....	44
Figure 2.2 Co-localization of Xin and MyoD at 24 hours of skeletal muscle regeneration.....	45
Figure 2.3 Xin-shRNA infection impairs skeletal muscle repair.....	46
Figure 2.4 Repression of Xin impairs satellite cell activation.....	48

CHAPTER 3

Figure 3.1 Xin ^{-/-} TA muscle exhibits morphologic differences in fiber area and fiber type compared to WT.....	76
Figure 3.2 Skeletal muscle regeneration following cardiotoxin injury is impaired in Xin ^{-/-} mice.....	78
Figure 3.3 Xin ^{-/-} satellite cells are hyperactivated compared to WT.....	79
Figure 3.4 Satellite cell/myoblast proliferative capacity is reduced in Xin ^{-/-} mice.....	81

CHAPTER 4

Figure 4.1 Muscle damage scoring system.....	103
Figure 4.2 Correlation between proteins of interest and degree of muscle damage in myopathic patients.....	104
Figure 4.3 Xin, Collagen, Filamin-C and Xirp2 display differential expression patterns as muscle damage increases.....	105
Figure 4.4 Xin expression in eccentrically damaged muscle from healthy subjects.....	106
Supplementary Figure 4.1 Xin expression in myopathic muscle grouped by disease.....	107
Supplementary Table 4.1 Summary of subject profile.....	108

LIST OF ABBREVIATIONS

ANOVA:	analysis of variance
AU:	arbitrary units
BrdU:	5-bromo-2-deoxyuridine
CTX:	cardiotoxin
DAPI:	4,6- diamidino-2-phenylindole
DMD:	Duchenne Muscular Dystrophy
ECM:	extracellular matrix
EDL:	extensor digitorum longus
FSHMD:	facioscapulohumeral muscular dystrophy
GAPDH:	glyceraldehyde-3-phosphate dehydrogenase
GPS:	gastrocnemius-plantaris-soleus complex
H&E:	hematoxylin and eosin
HGF:	hepatocyte growth factor
ICD:	intercalated disc
LGMD:	limb-girdle muscular dystrophy
MFM:	myofibrillar myopathy
MTJ:	myotendinous junction
Myh3:	embryonic myosin heavy chain
MyHC:	myosin heavy chain

NO:	nitric oxide
PFA:	paraformaldehyde
SC:	satellite cell
TA:	tibialis anterior
VASP:	vasodilator-stimulated phosphoprotein
WT:	wild type
Xin-/-:	Xin-deficient
XIRP1:	Xin-repeat protein 1 (encodes Xin)
XIRP2:	Xin-repeat protein 2 (encodes Xirp2)

Chapter 1: INTRODUCTION

Skeletal muscle has the remarkable capacity for rapid and extensive regeneration following injury. The major events that occur during muscle degeneration in response to stressors and subsequent regeneration are well-defined, however the underlying mechanisms that govern this process are less clear. The muscle stem cell population, termed satellite cells (SCs) play a key role in the regenerative process, as they become activated and enter the cell cycle in response to muscle damage. Upon activation, SCs have the capacity to proliferate and differentiate forming new muscle fibers, or repairing existing damaged myofibers until overall muscle morphology is restored. The progression of the SC through the cell cycle is regulated by key known myogenic factors, however many molecular factors have yet to be determined.

Recently, in attempt to determine novel factors involved in skeletal muscle regeneration, mRNA encoding the protein Xin was found to be highly upregulated early in the regenerative process, and localized to the SC population. Xin is a striated-muscle specific cytoskeletal protein that is found in the intercalated discs of the heart, and myotendinous junction of uninjured skeletal muscle. However, in response to damage, this expression profile changes drastically for reasons unknown. For example, in patients with various myopathies such as muscular dystrophy, skeletal muscle is constantly undergoing regeneration, and Xin expression is shown to be upregulated. Therefore, determining the reason for Xin upregulation during muscle repair is critical in the fundamental understanding of normal and diseased muscle regeneration, and associated SC function.

Skeletal Muscle Repair

Adult skeletal muscle is a stable tissue, consisting of muscle fibers, connective tissue and extensive vasculature. Upon injury, skeletal muscle has the capacity for extensive and rapid muscle repair, a process that is characterized by initial muscle degeneration, followed by the regeneration of myofibers (3), explained in further detail below. Briefly, during the initial phase of muscle repair, necrosis of muscle tissue occurs and the activation of an inflammatory response ensues. After which, the regeneration of muscle fibers is achieved by the activation of muscle stem cells (satellite cells; SCs) to proliferate and differentiate, thereby forming new myofibers, or repairing damaged fibers. Revascularization, reinnervation, and reconstitution of the extra-cellular matrix (ECM) are also important to the muscle regenerative process (3), however will not be the focus of this review.

Degeneration

During the degenerative phase, the onset of myofiber necrosis occurs rapidly. In a cardiotoxin injury model, which results in 80-90% of muscle degeneration, necrosis is observed within 12 hrs of cardiotoxin injury in mouse skeletal muscle (19). This is characterized by the disruption of myofiber sarcolemma, leading to myofiber permeability. Given the large disruptions in membrane permeability, levels of intracellular muscle proteins such as creatine kinase and myoglobin are increased in the sera. As these proteins are undetectable in subjects with no muscle damage, their increased presence in the sera are used as a measure of the amount of muscle damage in

subjects injured by extensive exercise, or muscle diseases such as muscular dystrophies (32).

Another hallmark of the initial phase of muscle injury is the induction of the inflammatory response, where cytokines and growth factors are released from damaged blood vessels to stimulate the migration of inflammatory cells to the site of injury (25). These inflammatory cells are important in the regulation of muscle regeneration as they impact muscle-specific gene expression and myofiber formation, demonstrated by the impairment of muscle repair after inducing monocyte/macrophage apoptosis (36). Also, studies of Duchenne Muscular Dystrophy (DMD) or the mdx mouse model of DMD, implicate immune elements such as lymphocytes, mast cells, eosinophils in the regenerative process, with neutrophils and macrophages being the dominating cell types (2, 38). Specifically, neutrophils are the first cell type to invade muscle 1-6 hrs after damage to phagocytose cellular debris, followed by an influx of macrophages after 48 hrs (3, 19, 21). Pro-inflammatory (M_1) macrophages phagocytose cellular debris such as myofilaments, cytosolic structures, and damaged sarcolemma. They also play a role in extending SC (myoblast) proliferation and delaying myoblast differentiation (2). Anti-inflammatory (M_2) macrophages are important in ECM deposition of collagen, fibronectin, laminin and proteoglycans through the activation of fibroblasts (25), thereby promoting the remodelling of muscle structure. Therefore, the histopathological characteristics of early muscle regeneration are muscle fiber necrosis, and the influx of non-muscle mononucleated cells.

Regeneration

After the initiation of the inflammatory response following injury, muscle regeneration and growth occurs. However, it is important to note that both these processes occur simultaneously. For example, it is during the initial inflammatory response when ECM remodelling begins, providing structural stability as damaged muscle fibers undergo phagocytosis. As such, an increase of ECM proteins such as collagen type I and III, laminin, fibronectin and proteoglycans occur through the migration and proliferation of fibroblasts (23, 25). Also, muscle degeneration and regeneration are mechanistically related, such as the influence of macrophage-induced cytokines on SC regulation (27), mentioned above.

Satellite cells are the stem cell population of skeletal muscle and play a key role in the regenerative process. They reside at the periphery of myofibers in a quiescent state, and become activated in response to muscle trauma. At which point they proliferate to form progeny termed myoblasts. Myoblasts differentiate to form new muscle fibers or fuse to pre-existing damaged fibers in attempt to repair them (19). The stages of satellite cell activation, proliferation, and differentiation will be discussed further in the next section.

Once myoblasts differentiate (myocytes), myofiber growth occurs, where myofibrillar assembly is important. Myofibrils are located within myofibers and are responsible for generating movement of skeletal muscle. They are comprised of repeating sarcomeric subunits of actin and myosin contractile units, anchored together by Z-discs. The organization of these contractile units is implicated as soon as 12 hours after injury in the

activated SC (40). Upon SC fusion (myocytes), the development of sarcomeres into mature myofibrils requires the assembly of numerous proteins, including scaffolding and chaperone adaptor proteins (10).

Newly formed myofibers are basophilic, and express developmental forms of myosin heavy chain such as embryonic myosin heavy chain (Myh3)(13), which is predominant within 5 days of muscle repair following cardiotoxin injury (19). Also characteristic of regenerating fibers is centrally located myonuclei, demonstrating the fusion of myoblasts to damaged fibers or to each other to form a new myofiber. Once fusion of myoblasts is completed, fibers increase further in size while replacing immature contractile proteins such as Myh3 with mature isoforms. Myonuclei migrate to the fiber periphery, and the muscle is functionally identical to undamaged muscle (4).

Various experimental models of muscle injury have been utilized to initiate processes of degeneration and regeneration in skeletal muscle. Methods include crush injury, usually used to examine regeneration in a confined region of muscle (24), and freeze lesions of superficial myofibers (11). A chemically induced method proven to induce extensive and reproducible skeletal muscle injury is cardiotoxin (CTX; purified *Naja nigricollis* snake venom) (12). The intramuscular injection of 10 μ M CTX into mouse hindlimb muscles result in 80-90% muscle degeneration, and therefore mostly de novo myofiber formation occurs (19, 23, 28). Within 6 hours of CTX injury, SCs become activated (19), proliferate by 2-3 days, and within 5 days form differentiated myotubes with a central nucleus (14). The myofibers grow, and by 10 days after CTX-induced injury, muscle

morphology is restored, however fibers are smaller than pre-injury size and still contain central nuclei (19).

Satellite Cells

Adult skeletal muscle contains cell populations with stem cell characteristics: the ability to differentiate into different cell lineages and self-renew. The primary stem cell population of skeletal muscle was first discovered in 1961 using electron microscopy (26). They reside at the myofiber periphery, under the basal lamina of each myofiber and in a relatively quiescent state, and account for about 2-4% of muscle nuclei. Quiescent SCs contain a high nuclear-to-cytoplasmic ratio, and can be identified with markers such as Pax7, M-cadherin, CD34 and Syndecan-4 (6, 18-20). SCs are important in the maintenance and regeneration of skeletal muscle, where in response to physiological stressors, they become activated and enter the cell cycle. After which, the cells will proliferate, at which point they are termed myoblasts, and migrate to the site of injury to repair or replace damaged myofibers. Damaged myofibers are regenerated through the fusion, and therefore differentiation of myoblasts, allowing for growth in fiber size (17). Even though the basic cell cycle regulatory processes has been noted in literature, the molecular mechanisms in place throughout cell activation, proliferation and differentiation are largely unknown.

Activation

The morphology of an activated SC differs from that of quiescent cells, marked by hypertrophied organelles and expanded cytoplasm (increased cytoplasm:nuclear ratio)

(1). These features can be used to determine a SC that has exited G₀, along with the upregulation of primary myogenic regulatory factors: MyoD and Myf5. The expression of MyoD occurs early after injury (within 6 hrs) and promotes SC progression to terminal differentiation, where Myf5 promotes SC self-renewal (16, 19). The incorporation of BrdU into newly synthesized DNA is also used to mark activation, although this requires entry into S-phase (43). One of the earliest markers used to determine SC activation is the colocalization of c-met with HGF (1). Whereby in response to stressors there is an influx of calcium ions which interact with calmodulin, resulting in nitric oxide (NO) radical production and matrix metalloproteinase activity. This in turn releases HGF from its extracellular tethering, although it is also suggested HGF can be released through an NO-independent pathway. The binding of HGF to SC surface receptor c-met activates the MAPK and PI3K pathways. These pathways result in the transcription of genes necessary for cell growth and division, as well as cell migration. (1, 9, 34, 37, 43). Once activated, SCs will emerge from underneath the basal lamina, migrating to the site of injury along the same myofiber, or to adjacent myofibers through tissue bridges to participate in the repair process (33, 34).

Proliferation and Differentiation

SC proliferation and subsequent differentiation into myotubes is regulated by various growth factors. Cellular proliferation is promoted by cytokines such as FGF, IGF-I, IGF-II and LIF, and attenuated by TGF- β (17). Early in the regenerative process, Notch signalling is required for satellite cell proliferation, which then switches to Wnt signalling during differentiation (6). Growth factors that promote differentiation include IGF-I and

IGF-II, whereas HGF, FGF and TGF-B inhibit this process (19). Also, studies indicate reduced muscle regenerative capacity when cellular proliferation is inhibited after exposure to colchicines, which inhibits cellular mitotic division (3). The upregulation of secondary myogenic regulatory factors (myogenin and MRF4) induces terminal differentiation of myoblasts into mononucleated myocytes, eventually leading to mature contracting fibers which express MyHC and creatine kinase (21). It is important to note that our full mechanistic insight into the pathways that allow for normal satellite cell activation, proliferation and differentiation at the molecular level is largely unknown. However, it is evident that the failure of each stage to occur results in aberrant skeletal muscle regeneration.

Xin

Localization and Structure

Xin is a striated muscle-specific cytoskeletal protein that is encoded by the gene Xin-repeat protein 1 (XIRP1), which consists of two exons. Splicing of these exons leads to three Xin isoforms: XinA (full length protein), XinB (carboxy-terminally truncated), and XinC (amino-terminally truncated) (39). Characteristic of this protein is its ability to bind actin filaments by its 16 Xin repeats, which are proposed to organize microfilaments into networks. Similar repeats were also found in 'Xin-repeat protein 2' (XIRP2), which contains 28 Xin repeats. Therefore these two proteins constitute the family of actin-binding proteins (31). Xin was discovered in 1996, when it was found to be expressed during early stages of cardiac development, where it plays a role in cardiac

morphogenesis (41, 42). In the adult, Xin is localized to the intercalated discs (ICD) of the heart, and myotendinous junctions (MTJ) in skeletal muscle, where it is believed to play a role in the organization of the actin cytoskeleton in areas of high mechanical stress (35). In skeletal muscle, Xin has been shown to interact with F-actin, Filamin-C, and Mena/vasodilator-stimulated phosphoprotein (VASP). Mena/VASP are members of protein family that are associated with regulating the actin cytoskeleton, and Filamin-C is a muscle specific protein that is involved in myofibril assembly and signaling between myofibril and the sarcolemma. (31, 39). The Xin protein contains many binding domains, however the purpose of these domains, especially in skeletal muscle is largely unknown. Identified domains include a proline-rich region, potential DNA binding and nuclear localization signal (NLS) domains, β -catenin binding region, Src homology 3 (SH3) binding motif, and 16 amino acid repeating units (Xin repeats) (5, 31, 39). .

Xin and skeletal muscle regeneration

Skeletal muscle has the ability to respond to injury and repair, largely due to its resident satellite cell population (19). Microarray analysis was utilized to identify novel factors involved in the regenerative process, and Xin mRNA was observed to be highly upregulated as early as 6 hrs, with peak levels 12 hrs after cardiotoxin injury. This finding was significant, as Xin mRNA in uninjured muscle is low, and resulting protein expression is only localized to the MTJ (18). In situ hybridization showed that Xin mRNA was also localized to areas consistent with satellite cells (18).

Immunohistochemical staining of isolated single fibers confirmed the expression of Xin within SCs, as it was colocalized with Syndecan-4, a known satellite cell marker (8, 18).

The observation of Xin upregulation after muscle injury was confirmed in a recent study on zebra fish by Otten et al (2012) (29). The same group have developed a novel Xin-deficient mouse model, where all three Xin isoforms are deleted (30). These animals develop normally and display only a mild cardiac phenotype. Isolated cardiomyocytes have mislocalized ICDs but no changes in the organization of myofibrils and no ultrastructural abnormalities, likely due to the presence of a compensatory mechanism. A Xin-deficient mouse model by another group revealed cardiac hypertrophy, fibrosis, ICD disruption, altered connexin-43, and likely compensation due to an upregulation of Xirp2 (15). The skeletal muscles of Xin-deficient mice have yet to be explored.

Regeneration and Myopathy

Most myopathies result from either a genetic mutation or chronic condition that affects skeletal muscle structural or cytoskeletal proteins, and morphology. One example of this is DMD, which is a devastating disease caused by an X-linked mutation of the cytoskeletal protein, dystrophin. The result is widespread degeneration of myofibers in response to mechanical stressors as the absence of the cytoskeletal protein reduces myofiber structural integrity. Therefore, DMD skeletal muscle is continuously going through bouts of degeneration and regeneration, ultimately exhausting the satellite cell pool, resulting in muscle fibrosis (19). Likewise, many other myopathies, such as limb girdle muscular dystrophies (LGMD), and inflammatory myopathy are characterized by the cycle of fiber necrosis and regeneration (6)(25).

In the regeneration of normal skeletal muscle, damaged myofibers are first removed by inflammatory cells, and then replaced by the differentiation of satellite cell progeny

(myoblasts). However in myopathic muscle, newly regenerated fibers are also prone to degeneration as a result of a molecular defect. Also, in diseased muscle, there is a persistent presence of macrophages, which modifies regulatory factors involved in muscle repair. Therefore the constant cycle of degeneration either exhausts the satellite cell population, or displays reduced myogenic potential, resulting in excess ECM accumulation and muscle replacement with adipose or fibrotic tissue (25). This process eventually leads to significant alterations in muscle structure, where variation in fiber size, forked fibers, and scattered myofibers are evident (6).

Human studies indicate that Xin is highly expressed in myofibrillar myopathies (MFM), which is defined by myofibril dissolution, degradation, and ectopic protein accumulation (7). One such mutation that can cause a MFM is of the Filamin-C gene. Filamins are a large group of cytoskeletal proteins which cross-link F-actin. Filamin-C is the muscle-specific filamin, and is localized to the z-disc, as well as the MTJ where it interacts with Xin. This myopathy is characterized by focal myofibrillar destruction, and Filamin-C containing aggregates within skeletal muscle fibers, which also contains Desmin, Myotilin, Dystrophin, Sarcoglycans, and Xin (22). However the role of Xin within damaged muscle fiber aggregates has yet to be determined. These findings, along with the knowledge of Xin upregulation during muscle regeneration suggests that Xin expression may be increased in other forms of myopathy.

Conclusion

In response to damage, adult skeletal muscle possesses the capacity to regenerate by repairing or assembling new myofibers. Fundamental to this process is the resident SC population, which becomes activated in response to stressors. Although the basic mechanisms of these processes have been defined in literature, many of the molecular changes that occur during satellite cell activation and skeletal muscle regeneration have yet to be determined.

Xin, a cytoskeletal actin-binding protein, has been shown to be highly upregulated early in the regenerative process, and localized to the SC population. However, in resting skeletal muscle, Xin expression is confined to the MTJ. Therefore, determining the role of Xin within regeneration will aid to elucidate specific molecular processes occurring during muscle repair, and within SCs. Interestingly, since Xin expression is upregulated during muscle repair, its expression within human myopathic disease which undergoes constant regeneration may be clinically relevant.

References

1. **Anderson JE.** A role for nitric oxide in muscle repair: nitric oxide-mediated activation of muscle satellite cells. *Mol Biol Cell* 11: 5: 1859-1874, 2000.
2. **Bencze M, Negroni E, Vallese D, Yacoub-Youssef H, Chaouch S, Wolff A, Aamiri A, Di Santo JP, Chazaud B, Butler-Browne G, Savino W, Mouly V and Riederer I.** Proinflammatory macrophages enhance the regenerative capacity of human myoblasts by modifying their kinetics of proliferation and differentiation. *Mol Ther* 20: 11: 2168-2179, 2012.
3. **Charge SB and Rudnicki MA.** Cellular and molecular regulation of muscle regeneration *Physiol Rev* 84: 1: 209-238, 2004.
4. **Charge SB and Rudnicki MA.** Cellular and molecular regulation of muscle regeneration. *Physiol Rev* 84: 1: 209-238, 2004.
5. **Choi S, Gustafson-Wagner EA, Wang Q, Harlan SM, Sinn HW, Lin JL and Lin JJ.** The intercalated disk protein, mXinalpha, is capable of interacting with beta-catenin and bundling actin filaments [corrected]. *J Biol Chem* 282: 49: 36024-36036, 2007.
6. **Ciciliot S and Schiaffino S.** Regeneration of mammalian skeletal muscle. Basic mechanisms and clinical implications. *Curr Pharm Des* 16: 8: 906-914, 2010.
7. **Claeys KG, van der Ven PF, Behin A, Stojkovic T, Eymard B, Dubourg O, Laforet P, Faulkner G, Richard P, Vicart P, Romero NB, Stoltenburg G, Udd B,**

Fardeau M, Voit T and Furst DO. Differential involvement of sarcomeric proteins in myofibrillar myopathies: a morphological and immunohistochemical study. *Acta Neuropathol* 117: 3: 293-307, 2009.

8. **Cornelison DD, Filla MS, Stanley HM, Rapraeger AC and Olwin BB.** Syndecan-3 and syndecan-4 specifically mark skeletal muscle satellite cells and are implicated in satellite cell maintenance and muscle regeneration. *Dev Biol* 239: 1: 79-94, 2001.

9. **Cornelison DD and Wold BJ.** Single-cell analysis of regulatory gene expression in quiescent and activated mouse skeletal muscle satellite cells. *Dev Biol* 191: 2: 270-283, 1997.

10. **Crawford GL and Horowitz R.** Scaffolds and chaperones in myofibril assembly: putting the striations in striated muscle. *Biophys Rev* 3: 1: 25-32, 2011.

11. **Creuzet S, Lescaudron L, Li Z and Fontaine-Perus J.** MyoD, myogenin, and desmin-nls-lacZ transgene emphasize the distinct patterns of satellite cell activation in growth and regeneration. *Exp Cell Res* 243: 2: 241-253, 1998.

12. **Doroshov JH, Tallent C and Schechter JE.** Ultrastructural features of Adriamycin-induced skeletal and cardiac muscle toxicity. *Am J Pathol* 118: 2: 288-297, 1985.

13. **Gambke B and Rubinstein NA.** A monoclonal antibody to the embryonic myosin heavy chain of rat skeletal muscle. *J Biol Chem* 259: 19: 12092-12100, 1984.

14. **Garry DJ, Meeson A, Elterman J, Zhao Y, Yang P, Bassel-Duby R and Williams RS.** Myogenic stem cell function is impaired in mice lacking the forkhead/winged helix protein MNF. *Proc Natl Acad Sci U S A* 97: 10: 5416-5421, 2000.
15. **Gustafson-Wagner EA, Sinn HW, Chen YL, Wang DZ, Reiter RS, Lin JL, Yang B, Williamson RA, Chen J, Lin CI and Lin JJ.** Loss of mXalpha, an intercalated disk protein, results in cardiac hypertrophy and cardiomyopathy with conduction defects. *Am J Physiol Heart Circ Physiol* 293: 5: H2680-92, 2007.
16. **Hagege AA, Vilquin JT, Bruneval P and Menasche P.** Regeneration of the myocardium: a new role in the treatment of ischemic heart disease? *Hypertension* 38: 6: 1413-1415, 2001.
17. **Hawke TJ.** Muscle stem cells and exercise training. *Exerc Sport Sci Rev* 33: 2: 63-68, 2005.
18. **Hawke TJ, Atkinson DJ, Kanatous SB, Van der Ven PF, Goetsch SC and Garry DJ.** Xin, an actin binding protein, is expressed within muscle satellite cells and newly regenerated skeletal muscle fibers. *Am J Physiol Cell Physiol* 293: 5: C1636-44, 2007.
19. **Hawke TJ and Garry DJ.** Myogenic satellite cells: physiology to molecular biology. *J Appl Physiol* 91: 2: 534-551, 2001.

20. **Hawke TJ, Kanatous SB, Martin CM, Goetsch SC and Garry DJ.** Rad is temporally regulated within myogenic progenitor cells during skeletal muscle regeneration. *Am J Physiol Cell Physiol* 290: 2: C379-87, 2006.
21. **Karalaki M, Fili S, Philippou A and Koutsilieris M.** Muscle regeneration: cellular and molecular events. *In Vivo* 23: 5: 779-796, 2009.
22. **Kley RA, Hellenbroich Y, van der Ven PF, Furst DO, Huebner A, Bruchertseifer V, Peters SA, Heyer CM, Kirschner J, Schroder R, Fischer D, Muller K, Tolksdorf K, Eger K, Germing A, Brodherr T, Reum C, Walter MC, Lochmuller H, Ketelsen UP and Vorgerd M.** Clinical and morphological phenotype of the filamin myopathy: a study of 31 German patients. *Brain* 130: Pt 12: 3250-3264, 2007.
23. **Krause MP, Moradi J, Nissar AA, Riddell MC and Hawke TJ.** Inhibition of plasminogen activator inhibitor-1 restores skeletal muscle regeneration in untreated type 1 diabetic mice. *Diabetes* 60: 7: 1964-1972, 2011.
24. **Kurek JB, Bower JJ, Romanella M, Koentgen F, Murphy M and Austin L.** The role of leukemia inhibitory factor in skeletal muscle regeneration. *Muscle Nerve* 20: 7: 815-822, 1997.
25. **Mann CJ, Perdiguero E, Kharraz Y, Aguilar S, Pessina P, Serrano AL and Munoz-Canoves P.** Aberrant repair and fibrosis development in skeletal muscle. *Skelet Muscle* 1: 1: 21, 2011.

26. **MAURO A.** Satellite cell of skeletal muscle fibers. *J Biophys Biochem Cytol* 9: 493-495, 1961.
27. **Nathan CF.** Secretory products of macrophages. *J Clin Invest* 79: 2: 319-326, 1987.
28. **Nissar AA, Zemanek B, Labatia R, Atkinson DJ, van der Ven PF, Furst DO and Hawke TJ.** Skeletal muscle regeneration is delayed by reduction in Xin expression: consequence of impaired satellite cell activation? *Am J Physiol Cell Physiol* 302: 1: C220-7, 2012.
29. **Otten C, van der Ven PF, Lewrenz I, Paul S, Steinhagen A, Busch-Nentwich E, Eichhorst J, Wiesner B, Stemple D, Strahle U, Furst DO and Abdelilah-Seyfried S.** Xirp proteins mark injured skeletal muscle in zebrafish. *PLoS One* 7: 2: e31041, 2012.
30. **Otten J, van der Ven PF, Vakeel P, Eulitz S, Kirfel G, Brandau O, Boesl M, Schrickel JW, Linhart M, Hayess K, Naya FJ, Milting H, Meyer R and Furst DO.** Complete loss of murine Xin results in a mild cardiac phenotype with altered distribution of intercalated discs. *Cardiovasc Res* 85: 4: 739-750, 2010.
31. **Pacholsky D, Vakeel P, Himmel M, Lowe T, Stradal T, Rottner K, Furst DO and van der Ven PF.** Xin repeats define a novel actin-binding motif. *J Cell Sci* 117: Pt 22: 5257-5268, 2004.
32. **Percy ME, Andrews DF and Thompson MW.** Duchenne muscular dystrophy carrier detection using logistic discrimination: serum creatine kinase, hemopexin,

pyruvate kinase, and lactate dehydrogenase in combination. *Am J Med Genet* 13: 1: 27-38, 1982.

33. **Schultz E and McCormick KM.** Skeletal muscle satellite cells. *Rev Physiol Biochem Pharmacol* 123: 213-257, 1994.

34. **Siegel AL, Atchison K, Fisher KE, Davis GE and Cornelison DD.** 3D timelapse analysis of muscle satellite cell motility. *Stem Cells* 27: 10: 2527-2538, 2009.

35. **Sinn HW, Balsamo J, Lilien J and Lin JJ.** Localization of the novel Xin protein to the adherens junction complex in cardiac and skeletal muscle during development. *Dev Dyn* 225: 1: 1-13, 2002.

36. **Summan M, Warren GL, Mercer RR, Chapman R, Hulderman T, Van Rooijen N and Simeonova PP.** Macrophages and skeletal muscle regeneration: a clodronate-containing liposome depletion study. *Am J Physiol Regul Integr Comp Physiol* 290: 6: R1488-95, 2006.

37. **Tatsumi R.** Mechano-biology of skeletal muscle hypertrophy and regeneration: possible mechanism of stretch-induced activation of resident myogenic stem cells. *Anim Sci J* 81: 1: 11-20, 2010.

38. **Tidball JG.** Inflammatory processes in muscle injury and repair. *Am J Physiol Regul Integr Comp Physiol* 288: 2: R345-53, 2005.

39. **van der Ven PF, Ehler E, Vakeel P, Eulitz S, Schenk JA, Milting H, Micheel B and Furst DO.** Unusual splicing events result in distinct Xin isoforms that associate differentially with filamin c and Mena/VASP. *Exp Cell Res* 312: 11: 2154-2167, 2006.
40. **Vater R, Cullen MJ and Harris JB.** The expression of vimentin in satellite cells of regenerating skeletal muscle in vivo. *Histochem J* 26: 12: 916-928, 1994.
41. **Wang DZ, Hu X, Lin JL, Kitten GT, Solorsh M and Lin JJ.** Differential displaying of mRNAs from the atrioventricular region of developing chicken hearts at stages 15 and 21. *Front Biosci* 1: a1-15, 1996.
42. **Wang DZ, Reiter RS, Lin JL, Wang Q, Williams HS, Krob SL, Schultheiss TM, Evans S and Lin JJ.** Requirement of a novel gene, Xin, in cardiac morphogenesis. *Development* 126: 6: 1281-1294, 1999.
43. **Wozniak AC, Kong J, Bock E, Pilipowicz O and Anderson JE.** Signaling satellite-cell activation in skeletal muscle: markers, models, stretch, and potential alternate pathways. *Muscle Nerve* 31: 3: 283-300, 2005.

Chapter 2: PREFACE

Significance to thesis

The primary goal of this study was to determine the contribution of Xin to the skeletal muscle repair process. The overall stages of muscle repair is well-defined in literature, however the underlying mechanisms driving these processes are not as clear. Therefore it was important to determine the relevance of Xin mRNA upregulation in early muscle regeneration, and if it translates to protein expression. The first aim of this study was to characterize Xin protein expression within skeletal muscle throughout the regenerative timecourse after cardiotoxin injury. Also, Xin was previously found to be localized to satellite cells which are fundamental to skeletal muscle repair. Therefore the second aim of this study was to determine the role of Xin in regulating satellite cell activation and proliferation. The method used to determine the functional contribution of Xin to skeletal muscle repair and satellite cell function was Xin-shRNA adenoviruses, which selectively targets Xin-expressing cells. This method was previously shown to reduce endogenous Xin levels by ~60%, therefore any alterations to satellite cell function and ultimately skeletal muscle repair compared to control muscle can be attributed to the reduction of Xin.

Contribution of Authors

Aliyah A. Nissar contributed to the data shown in Figure 1 and Figure 2, assessed Myh3 expression, wrote the initial draft of the manuscript, and worked on revising the draft based on editorial review.

Bart Zemanek, Rita Labatia, and Daniel J. Atkinson contributed to the data shown in Figure 3 and Figure 4.

Peter F. M. van der Ven and Dieter O. Fürst contributed to the design of the study, supplied proprietary reagents and edited the manuscript.

Thomas J. Hawke designed the study, assisted in experiments, edited the manuscript and funded the study.

Skeletal muscle regeneration is delayed by reduction in Xin expression: consequence of impaired satellite cell activation?

Aliyah A. Nissar^{1,2}, Bart Zemanek², Rita Labatia², Daniel J. Atkinson², Peter F. M. van der Ven³, Dieter O. Fürst³ and Thomas J. Hawke^{1,2}.

¹ Department of Pathology and Molecular Medicine, McMaster University. Hamilton, ON, Canada.

² Muscle Health Research Centre, York University, Toronto ON, Canada.

³ Institute for Cell Biology, University of Bonn. Bonn, Germany.

Running title: Xin is a critical protein in muscle repair.

Correspondence: Thomas J. Hawke, PhD

Department of Pathology & Molecular Medicine, McMaster University

1280 Main St West, Hamilton ON Canada. L8S 4L8

email: hawke@mcmaster.ca

phone: 905-525-9140 ext 22372

Abstract

Xin is a striated muscle-specific actin-binding protein whose mRNA expression has been observed in damaged skeletal muscle. Here we demonstrate increased Xin protein expression early post-injury (≤ 12 hours) and localization primarily to the periphery of damaged myofibers. At 1 day post-injury, Xin is co-localized with MyoD, confirming expression in activated satellite cells (SCs). By 5 days post-injury, Xin is evident in newly-regenerated myofibers, with a return to pre-injury levels by 14 days of regeneration.

To determine if the increased Xin expression is functionally relevant, tibialis anterior muscles of wild-type mice were infected with Xin-shRNA adenovirus, while the contralateral tibialis anterior received Control adenovirus (Control). Four days post-infection, muscles were harvested or injured with cardiotoxin and collected at 3, 5 or 14 days thereafter. Compared to Control, Xin-shRNA infection attenuated muscle regeneration as demonstrated by Myh3 expression and fiber areas. Given the co-localization of Xin and MyoD, we isolated single myofibers from infected muscles to investigate the effect of silencing Xin on SC function. Relative to Control, SC activation, but not proliferation, was significantly impaired in Xin-shRNA infected muscles. To determine if Xin affects the G0-G1 transition, cell cycle re-entry was assessed on infected C2C12 myoblasts using a methylcellulose assay. No difference in re-entry was noted between groups, suggesting that Xin contributes to SC activation by means other than affecting G0-G1 transition. Together these data demonstrate a critical role for Xin in SC activation and reduction in Xin expression results in attenuated skeletal muscle repair.

Introduction

While the ability for skeletal muscle to grow, adapt and regenerate is well known, the numerous factors governing this ability are less well defined. Furthermore, satellite cells, the primary stem cell of skeletal muscle, are critical to these capacities of skeletal muscle and the factors governing their regulation are still being uncovered. In previous work, we identified Xin to be highly upregulated at the mRNA level within regenerating skeletal muscle, particularly during the early phases of regeneration (10).

Xin was initially observed as a critical protein for heart looping in developing chick embryos. To date however, the role(s) within skeletal muscle for this striated muscle-specific, cytoskeletal protein, has yet to be elucidated. In developing mouse skeletal muscle, Xin can be detected within somites at embryonic day 10 (E10) and by E13.5, Xin is seen in some maturing skeletal muscle with expression expanding to include all skeletal muscles as the animal reaches maturity (10). That said, endogenous mRNA levels of Xin in healthy, uninjured, adult skeletal muscle are observed to be low (10) and protein expression appears to be primarily localized to the myotendinous junction (16). The mRNA expression within skeletal muscle changes dramatically in response to muscle injury, however, with increased Xin detected within 6 hours of damage and a peak in expression noted at 12 hours post-injury (10). Using in situ hybridization, the early expression of Xin mRNA was observed at the periphery of muscle fibers; an area consistent with the location of muscle satellite cells. Immunohistochemical staining of isolated single fibers confirmed the expression of Xin in satellite cells as it could be co-localized with Syndecan-4, a known satellite cell marker (6, 10).

While the expression of Xin mRNA has been demonstrated to be increased within damaged skeletal muscle (1, 2, 10), it was unknown if this translated to changes in protein expression, and whether these changes were functionally significant to the muscle repair process. As well, it had yet to be elucidated if the expression of Xin within the satellite cell was critical for the regulation of this stem cell population. Thus, the purpose of the present study was define the protein expression of Xin within regenerating muscle and then to determine the functional contribution of Xin to skeletal muscle repair and satellite cell function through the use of Xin-shRNA adenoviruses. The in vivo results of this work demonstrate that Xin-shRNA adenoviruses injected into skeletal muscle lead to delayed regeneration following injury as demonstrated by fiber area quantification and Myh3 (myosin heavy chain- embryonic isoform) expression. Our in vitro results demonstrate that reduced expression of Xin leads to an impairment in the ability of satellite cells to become ‘activated’, but does not affect their proliferative capacity. Taken together, the findings of the current study highlight Xin as a critical protein for satellite cell activation and reducing Xin expression during skeletal muscle repair attenuates the regenerative process.

Materials and Methods

Animals

Male C57Bl/6 mice (3-4 months of age) were obtained from Jackson Laboratories (Bar Harbor, ME). All mice had access to enrichment material (nesting material, cardboard tubing) and were provided with standard breeder chow and water *ad libitum*. Animals were housed in an environment maintained at 21°C, 50% humidity and 12h/12h light-dark cycle. All experimental protocols were approved by the York University and McMaster University Committees on Animal Care and performed in accordance with the Canadian Council Animal Care guidelines.

Adenoviral material

All adenoviral constructs were prepared by Vector Biolabs using Adenoviral vector Type 5 (www.vectorbiolabs.com), purified by CsCl centrifugation, and have been published previously (10). As previously noted, the Xin-shRNA adenovirus resulted in a greater than 50% decrease in Xin mRNA expression and an approximate 60% decrease in endogenous Xin, 4 days post-infection, compared to Control (10). Briefly, to decrease endogenous Xin levels, the right tibialis anterior (TA) muscle of each mouse was infected with an adenovirus containing Xin-shRNA, which also expressed GFP used to determine adenoviral infection efficiency: (Ad-CMV-Xin-shRNA-GFP; Loop sequence:

TTCAAGAGA; sense 5'-
GATCCGGAAGAAAAGGGATATCAGTTCAAGAGACTGATATCCCTTTTCTTCCT
TA-3'; antisense: 5'-

AGCTTAAGGAAGAAAAGGGATATCAGTCTCTTGAAGTATATCCC
TTTTCTTCCG-3’).

The contralateral leg of each animal was used as a control and infected with the same adenoviral vector containing GFP alone (Ad-CMV-GFP). Injection into the muscles was done using a Hamilton syringe with the needle inserted at the distal tendon in a distal to proximal direction, along the length of the muscle belly. Once the needle was inserted, the adenovirus (4.7×10^{10} pfu suspended in a 2:1 adenovirus to PBS ratio by volume) was injected as the needle was slowly withdrawn (along the length of the muscle). In this way, approximately 75% of the muscle belly length was infected with similar degrees of infection observed between all mice regardless of vector. We estimated that approximately 35% of the muscle was infected by our injection strategy. This same procedure was undertaken to infect the EDL (deep and lateral to TA) and the lateral compartment (peroneus) muscles for single muscle fiber experiments. Only areas/fibers expressing GFP were used in our measurements.

Adenoviral infection efficiency within myoblasts, regardless of construct, was routinely greater than 90% such that any difference in expression noted is the result of the degree of Xin repression rather than the degree of infection efficiency.

Skeletal Muscle Injury

Skeletal muscle injuries were induced using a 100 μ L intramuscular injection of 10 μ M cardiotoxin (CTX; Latoxan, Valence, France), as previously described (10). To establish a timeline for Xin expression in regenerating muscle, TA muscles were harvested prior to

CTX injection (0 day), or at 0.5, 1, 3, 5 and 14 days post-injury (n=4: 0d, 1d, 3d, 5d; n=3: 0.5d, 14d). In the adenoviral experiments, CTX injury was induced four days following adenoviral infection in the left and right TA muscles. Muscles were harvested prior to injury (0d) or at 3, 5 and 14 days post-CTX injury.

Tissue collection

Animals were euthanized by CO₂ inhalation followed by cervical dislocation. The TA muscles were excised and cut transversely in half. The proximal half was snap-frozen in liquid nitrogen, whereas the distal half was coated in tissue mounting medium and frozen in liquid nitrogen-cooled isopentane. Uninjured (0d) left and right extensor digitorum longus (EDL) and peroneus longus muscles were harvested to isolate single muscle fibers.

Single muscle fiber isolation

Single muscle fibers were obtained from left (Control) and right (Xin-shRNA) EDL and peroneus muscles one day following adenoviral infection (n=5), as previously described (11). Briefly, muscles were removed and digested in a collagenase solution. Resulting muscle bundles were triturated to isolate single fibers that were then collected using a sterile glass Pasteur pipette, and placed in 24 well culture dishes containing plating media [10% normal horse serum, 0.5% chick embryo extract (MP Biomedicals, Ohio) in Dulbecco's Modified Essential Medium (DMEM; Invitrogen, USA)].

Satellite cell activation and proliferation analysis

Satellite cell activation was assessed in floating culture by adding 10 μ M 5-bromo-2-deoxyuridine (BrdU; Sigma 858811) to the plating media and incubating newly isolated single fibers for 24 hours. After this duration, fibers were fixed in 4% PFA, incubated in 2N HCl for 1 hour at 37°C, followed by blocking buffer (1.5% normal goat serum, 1.5% normal horse serum) for 1 hour. BrdU antibody (Sigma B2531) was diluted 1:25 in PBS and applied overnight at 4°C. A biotin/streptavidin (Vector Labs) detection system was used to visualize BrdU⁺ satellite cells, and propidium iodide to stain all nuclei. Satellite cells that became activated and entered the cell cycle incorporated BrdU; therefore activation was analyzed by the number of BrdU positive cells per muscle fiber (20).

Satellite cell activation was also assessed by infecting single fibers isolated from C57Bl/6 mice with 1 μ l of 1x10¹⁰/ml of either the Xin-shRNA Ad or GFP Ad constructs in matrigel-coated plates to allow fibers to adhere. Fibers were left undisturbed for 24 hour, after which the number of myoblasts which had migrated away from the fiber was determined using light microscopy. To assess proliferation, the same fibers were examined at 48 hours post plating and quantified for number of myoblasts present and again at 72 hours to determine the fold increase in cell doublings. A total of 50 fibers from an n=5 were analyzed for all Control and Xin-shRNA groups.

Western Blot Analysis

Proximal halves of TA muscles were ground in liquid nitrogen to a powder, which was then added to 2x SDS sample buffer, heated to 65°C for 15 min ensuring not to boil samples, and sonicated to shear DNA and homogenize (17). The protein was separated

using polyacrylamide gel electrophoresis, and transferred to a PVDF membrane as previously described (13). Primary antibodies for Xin (17) and MyoD (Dako) were used to detect proteins of interest. Protein expression was visualized by the binding of HRP-conjugated secondary antibodies, and the addition of Super Signal West Femto chemiluminescent reagent (Pierce Biotechnology Inc). The antibody used to detect Xin is directed towards the Xin-repeats, and thus detects both the A and B isoforms of Xin. As discussed later, Xin B was the primary isoform (~130 kDa) detected throughout these studies.

Images of blots were acquired with the Fusion Fx7 imager and accompanying software. Analysis of blots was performed using ImageJ freeware. It should be noted that significant changes in proteins normally used as loading controls (e.g. GAPDH) during skeletal muscle regeneration occur. Therefore, a Ponceau (Sigma P3504) stain was used to confirm equal protein loading and normalize the loading of left and right TA samples of the same animal for each specific time point. Thus, in Figure 2.3C, quantification is normalized for each time point, but not between time points.

Cell Cycle Arrest and Re-entry Assay

Control and Xin-shRNA infected C2C12 cells were trypsinized and suspended in a final concentration of 3×10^5 into cell culture flasks containing 2% methylcellulose (Methocel A4M Premium; Dow Chemicals) in serum-containing DMEM and incubated for 72 hours to ensure cell cycle arrest. Cells were recovered from the methylcellulose media by dilution in room temperature phosphate buffered saline (PBS), centrifugation, and PBS

washes. Cells were further cleaned by passing through sterile 70 μ m filters and a Ficoll gradient. Cells were then plated in proliferation medium (10% FBS, high glucose DMEM) and allowed to re-enter the cell cycle and proliferate for 12, 18 or 24 hour hours. After the allotted time, cells were detached by trypsinization, washed in PBS, fixed with 70% cold ethanol while being vortexed, and then resuspended in a propidium iodide / RNase A staining solution (1mg/ml propidium iodide, 2mg/ml RNase A) overnight to label DNA and degrade RNA. Using a Fluorescence-Activated Cell Sorter flow cytometer (BD FACSCalibur; BD Biosciences), 10,000 live events were acquired for each sample using Cellquest software (BD Biosciences). The percentage of cells in each phase of the cell cycle was quantified using ModFit LT for Mac v3.0 software as previously described (8).

Histochemical and Immunofluorescent Analyses

Distal TA muscles were transversely cut into 8 μ m sections and adhered to glass slides for subsequent histochemical or immunofluorescent staining.

Hematoxylin and Eosin (H&E) stain: H&E stains were used for the determination of Control and Xin-shRNA adenoviral infected TA fiber area at 5 and 14 days of regeneration. Greater than 100 injured fibers (GFP positive and centrally-located nuclei) throughout each muscle section were analyzed.

Immunofluorescent Staining: Embryonic myosin heavy chain (Myh3) expression was detected by immediately fixing cut sections in 2% PFA, incubating in block (10% normal goat serum and 1.5% bovine serum albumin) for 30 minutes followed by mouse IgG

block (Vector, BMK 2202) for 1 hour at room temperature. Sections were then incubated with undiluted Myh3 antibody (Hybridoma Bank F1.652) at 4°C overnight. To visualize Myh3, sections were incubated in Alexa 488 anti-mouse antibody for 1 hour at room temperature. A drop of 1:10000 4,6-diamidino-2-phenylindole (DAPI) was applied to the section for 5 minutes to identify nuclei. To validate our direct observations of adenoviral-mediated GFP expression using fluorescent microscopy, GFP expression within some infected muscle sections was also detected using a rabbit polyclonal antibody (Abcam ab290) and visualized with a Texas-Red conjugated secondary antibody.

Xin expression was detected by applying undiluted primary antibody (17) to the fixed section for 1 hour at room temperature, after the mouse IgG block. A biotin/streptavidin detection system was used as recommended (Vector Labs). The sections were then incubated in streptavidin antibody conjugated to Texas-Red diluted 1:100 for 30 minutes at room temperature. Blocking buffer was applied before co-staining with laminin (Abcam; ab14055) or MyoD antibodies (Abcam; ab64159), which were diluted 1:250 and incubated overnight at 4°C. To detect laminin and MyoD, Alexa 488 anti-chick and anti-rabbit antibodies were applied respectively to the muscle section, followed by DAPI.

Image analysis

Images of stained muscle sections were captured using a Nikon 90i eclipse upright microscope. Using Nikon Elements software, fiber areas were determined by manually outlining fibers, and Myh3 stains were analyzed using threshold detection for positive fibers.

Statistical Analysis

Student's *t* tests were performed to test for significant differences ($P < 0.05$) in data obtained from Xin-shRNA and Control muscles. Data are presented as means \pm standard error (S.E.).

Results

Protein expression of Xin is observed within satellite cells and regenerating muscle following injury

While it was previously demonstrated that Xin expression at the mRNA levels was observed in the regenerating muscle (via RT-PCR and in situ hybridizations), it remained unknown if this increase in mRNA translated into an increase in protein expression. As can be seen in Figure 2.1, the increase in Xin protein expression occurs within 12 hours following cardiotoxin-induced muscle damage and the intensity increases by 24 hours following injury, a finding consistent with an increase in mRNA at 6 and 12 hours following damage (10). Though the mRNA expression appeared to decrease by 3 days post-injury (2), Xin protein was clearly evident at 5 days post-injury within newly regenerated muscle fibers (as illustrated by the centrally-located nuclei). By 14 days of repair, the expression of Xin protein was very low, comparable to pre-injury (0 day) levels.

At 24 hours post-injury, the expression of Xin appeared in areas consistent with satellite cells (i.e. under the basal lamina and in association with nuclei; Figure 2.1). While this association was not unexpected based on our previous work (10), we had not yet demonstrated that Xin was definitively expressed in activated satellite cells/myoblasts at the protein level within damaged skeletal muscle. To confirm this, we co-stained 24 hour post-injury skeletal muscle samples with antibodies detecting Xin and the myogenic regulatory factor, MyoD (Figure 2.2). Some examples of this co-localization are shown

in Figure 2.2, supporting the hypothesis that Xin is expressed in activated satellite cells and its expression may be important in satellite cell function.

Repression of Xin in vivo leads to a delay in muscle repair

To investigate the function of Xin within regenerating skeletal muscle, we undertook an adenoviral-mediated approach to down-regulate Xin expression with one TA muscle receiving Xin-shRNA and the contralateral leg receiving the Control adenoviral vector (Figure 2.3). Western blotting analysis for Xin expression in Control and Xin-shRNA infected myoblasts demonstrated a ~60% decrease in endogenous Xin expression at 4 days post-infection (Figure 2.3A). This level of reduction is consistent with our in vivo repression level (0 day time point in Figure 2.3C). As illustrated in Figure 2.3B, both vectors contained GFP to allow for identification of infected areas. To verify the presence of GFP within the regenerating muscle (and thus confirm the presence of the adenovirus/expression of shRNA while ruling out an autofluorescent component) we stained regenerating muscle (14 day) with anti-GFP and detected this with a secondary antibody conjugated to Texas Red secondary antibody. The infected area stained intensely for the presence of GFP protein even at 14 days of regeneration (18 days post-infection).

In Figure 2.3C, the effect of Xin-shRNA can be observed in resting and regenerating skeletal muscle. In Control infected muscles, Xin protein expression increased significantly in the first 12 hours of regeneration with a peak in expression at 24 hours. In contrast to our immunohistochemical observations, the expression of Xin (by

immunoblotting) returned to the uninjured levels by 3 days of regeneration and remained at that level through the remaining 11 days of repair. The Xin-shRNA adenovirus infection was successful in blunting the rise in Xin expression at 12 and 24 hours of regeneration. Interestingly, while the expression of Xin in Control muscles returned to the pre-injury state by 3 days of repair, the Xin-shRNA infected muscles displayed a continued presence of elevated Xin expression (albeit blunted). By 5 days of regeneration in the Xin-shRNA muscle, the expression of Xin is similar to Control levels and not until 14 days of repair does the expression return to levels significantly reduced compared to Control infected muscles.

At all time points of regeneration, the expression of Xin B (~130 kDa) was the dominant isoform of expression with only faint or absent signal detected at the level of Xin A (~205 kDa). Therefore, only the expression of Xin B is presented here and we hereafter refer to the Xin B isoform as Xin.

The expression of MyoD, a known transcriptional regulator of Xin (2), increases in both groups within hours of muscle damage, but only in the Xin-shRNA-infected muscle does the expression remain significantly elevated at 3 days post-injury (Figure 2.3C, lower panel). Thereafter, MyoD expression in the Xin-shRNA muscle decreases to be modestly, but significantly, elevated at 5 days before returning to Control levels at 14 days post-injury.

The robust expression of Xin during muscle regeneration suggests an important role for this striated muscle-specific protein in the repair process. The expression of myosin

heavy chain isoforms that are expressed only during defined periods of regeneration (e.g. embryonic myosin heavy chain; Myh3) is routinely used to illustrate alterations in the rate of skeletal muscle repair. We observed a significant reduction in the expression of Myh3 at 5 days of regeneration in the Xin-shRNA-infected muscles (Figure 2.3D; Xin-shRNA: $10.23 \pm 0.25\%$ vs. Control-GFP: $15.01 \pm 0.25\%$; N=3/group; P=0.0002). This result is consistent with our findings using muscle fiber area as a metric for myofiber maturation. When we quantified the areas of newly regenerating muscle fibers (GFP positive muscle fibers with central nuclei) in Xin-shRNA and Control-infected muscles at 5 and 14 days post-cardiotoxin injury we observed that the regenerating muscle fibers of Xin-shRNA-infected muscles are significantly smaller than the Control-infected contralateral muscles at both 5 and 14 days of repair (Figure 2.3D). Taken together, these results illustrate that, relative to Control adenovirus-infected muscles, there is a significant delay in the muscle repair process upon down-regulation of Xin expression.

Decreasing Xin expression in primary satellite cells impairs activation, but does not directly affect proliferation

Having detected the expression of Xin in activated satellite cells both *in vitro* (10) and within regenerating skeletal muscle (present study), as well as our finding that reducing endogenous Xin expression impaired skeletal muscle repair, we hypothesized that reducing endogenous Xin expression may be affecting satellite cell activation. An impairment in satellite cell activation may therefore account, at least in part, for the delay in muscle repair. To test this hypothesis, we infected the skeletal muscle (and associated

satellite cells) prior to the isolation of single fibers with our Control or Xin-shRNA adenoviruses. The isolation procedure for single myofibers results in the activation of the resident satellite cells (20). By incubating the newly isolated fibers in a floating culture with the thymidine-analogue BrdU, and assessing its incorporation within 24 hours of isolation, we obtain an estimate of the rate of satellite cell activation (20). Figure 2.4A illustrates a BrdU-positive satellite cell at the periphery of an isolated myofiber, 24 hours after isolation. When the number of BrdU-positive cells at the periphery of isolated myofibers are compared between Control and Xin-shRNA-infected groups, we see a significant (~50%) reduction in the number of BrdU-positive satellite cells in the presence of Xin-shRNA (Figure 2.4B). Another means to assess satellite cell activation is to quantify the number of satellite cells which migrate off the isolated myofibers in an ‘adherent-fiber’ preparation (11). Consistent with our BrdU-incorporation assay, the number of satellite cells which migrated off the myofiber onto the matrigel-coated plate was reduced by more than 60% upon infection of Xin-shRNA (Figure 2.4C).

Though we had previously demonstrated a small, but significant effect of Xin-shRNA on C2C12 myoblast proliferation (10), we did not observe any effect of Xin-shRNA on the proliferative capacity of primary myoblasts in culture (Figure 2.4D). This effect may be the result of inherent differences between primary and cell line cultures. For example, given the greater proliferative capacity of C2C12 cells, small differences in proliferative capacity may be amplified within the short assay time compared to the longer cell cycle times associated with newly isolated myoblasts (11).

As Xin is an actin-binding protein, we hypothesized that Xin's role in satellite cell activation was to contribute to the large increase in cell size needed to accommodate the cellular hypertrophy immediately following stimulation. However, it was also conceivable that it was playing a role modulating cell cycle progression (e.g. G0-G1 transition). To investigate this, we infected C2C12 cells with Xin-shRNA or Control adenoviruses and then rendered them quiescent through 72 h of culturing in a methylcellulose-supplemented medium (12, 15). We observed no significant difference between groups in their re-entry into the cell cycle at 12, 18 or 24 hours (Figure 2.4E) lending support to our hypothesis that Xin is involved in cytoskeletal remodeling during satellite cell activation, rather than directly affecting G0-G1 cell cycle transition.

Discussion

We had previously demonstrated a significant increase in the expression of Xin mRNA following skeletal muscle damage (10). At that point, however, it had remained unknown whether this expression pattern translated to significant changes in Xin protein levels and what the functional significance of Xin may be in muscle repair. In the present study, we substantiate a robust increase in Xin protein within hours of muscle damage, and many focal areas of Xin expression at these early stages of regeneration reveal co-localization with the myogenic regulatory factor, MyoD. The co-localization of Xin and MyoD support the presence of Xin in activated satellite cells early after muscle injury. Interestingly, the expression of Xin protein is also readily detected in newly regenerating muscle fibers by 5 days of repair. By 14 days of regeneration, Xin expression is low, comparable to that observed in uninjured skeletal muscle. We further demonstrate that a reduction in Xin expression in vivo, through the use of adenovirally-mediated Xin-shRNA, attenuates skeletal muscle regeneration as evidenced by reductions in the 5 day post-injury expression of Myh3 and reduced myofiber areas at 5 and 14 days post-injury. This effect appears to be mediated, at least in part, by an impairment in satellite cell activation. Taken together, these findings highlight a role for Xin within skeletal muscle repair, particularly within the resident muscle stem cell population.

An interesting observation from our immunohistochemical analysis in regenerating muscle is the apparent 'biphasic' nature of Xin expression. While this is not readily apparent with PCR (10) or immunoblotting (present study), visualization of Xin expression both at the mRNA level by in situ hybridization (10) or of the protein by

immunohistochemistry demonstrates an early expression phase (< 24 hours post-injury; particularly around the periphery of the muscle fibers) that is followed by a decrease in expression and subsequently by a second peak of expression (5-7 days) in small muscle fibers with centrally-located nuclei. The heterogeneous expression pattern of Xin within these newly-regenerated myofibers may reflect a temporal limitation of this study. That is, although Xin may be expressed in all regenerating fibers, because of the asynchrony of regeneration (and the limitation of harvesting at 0.5, 1, 3, 5 and 14 days), we may be only observing fibers that are expressing Xin at that specific time. While much of the early expression of Xin coincides with MyoD and represents the activated satellite cell population (5, 7), the purpose of the second phase of Xin expression is less clear. We hypothesize that this expression pattern may indicate a role for this cytoskeletal protein in myofibril assembly/formation, akin to that observed for other stress-fiber related proteins in cultured chick cardiac myocytes (9). If, as we propose, Xin is involved in myofibrillar assembly, the expression of Xin in the early phase of regeneration that does not co-localize with MyoD may represent immediate remodeling/repair of myofibrils in response to damage in some muscle fibers. Further investigations are obviously needed to test this hypothesis and clarify the purpose of Xin in the terminal differentiation of regenerating muscle fibers.

To reveal the importance of Xin for skeletal muscle repair, we utilized an adenoviral Xin-shRNA-mediated knockdown approach. We have previously proven the efficacy of this adenovirus in cell culture, but now also demonstrate an efficient knock-down of Xin expression levels in vivo. Although the injection of Xin-shRNA adenovirus did not result

in a complete absence of Xin expression as would be observed in a knockout mouse model, this technique did offer some important advantages: (i) injection of Xin-shRNA adenovirus into one muscle and the Control adenovirus into the contralateral muscle allowed to obtain an internal Control for each mouse; (ii) any systemic effect of adenoviral injection would affect both legs similarly; (iii) the use of adenoviruses into wild-type muscle should reduce the contributions of compensatory proteins that would arise during development (14).

The repression of Xin expression resulted in significant delays in muscle regeneration as demonstrated both by smaller muscle fiber sizes at 5 and 14 days post-injury and a reduction in the amount of embryonic myosin heavy chain at 5 days post-injury. While it could be speculated that the reduction in muscle fiber areas observed in regenerating Xin-shRNA muscles may be the result of the aforementioned proposed role for Xin in myofibril assembly (and thus muscle fiber hypertrophy), the expression of Xin within activated satellite cells and the decreased Myh3 expression lends more support to the hypothesis that the attenuated regeneration in Xin-shRNA skeletal muscle is, at least in part, the result of a delay in satellite cell activation.

Activation of the muscle satellite cell from a state of quiescence requires a number of coordinated events to allow the satellite cell to enter the proliferative phase (18, 20). Two major events occurring as the satellite cell becomes activated are (i) an increase in cytoskeletal remodeling requisite for the increased cell size and organelle content, as well as (ii) the G0 to G1 cell cycle phase transition (3, 4). The methylcellulose assay has been used extensively to research factors responsible for activation/cell cycle re-entry (8). The

use of C2C12 cells in this assay allowed us to dissociate the potential role(s) of Xin in cell cycle re-entry from a cytoskeletal remodeling role as these cells had been actively cycling prior to arrest. As we show in Figure 2.4E, there is no significant effect of repressing Xin expression on cell cycle re-entry as demonstrated using FACS analysis. While this supports the role for Xin in cytoskeletal remodeling, clearly future studies will be needed to investigate how Xin may be mediating this effect.

In conclusion, these findings contribute to our understanding of Xin within skeletal muscle, particularly as an integral protein in skeletal muscle regeneration possibly through its role in activating satellite cells.

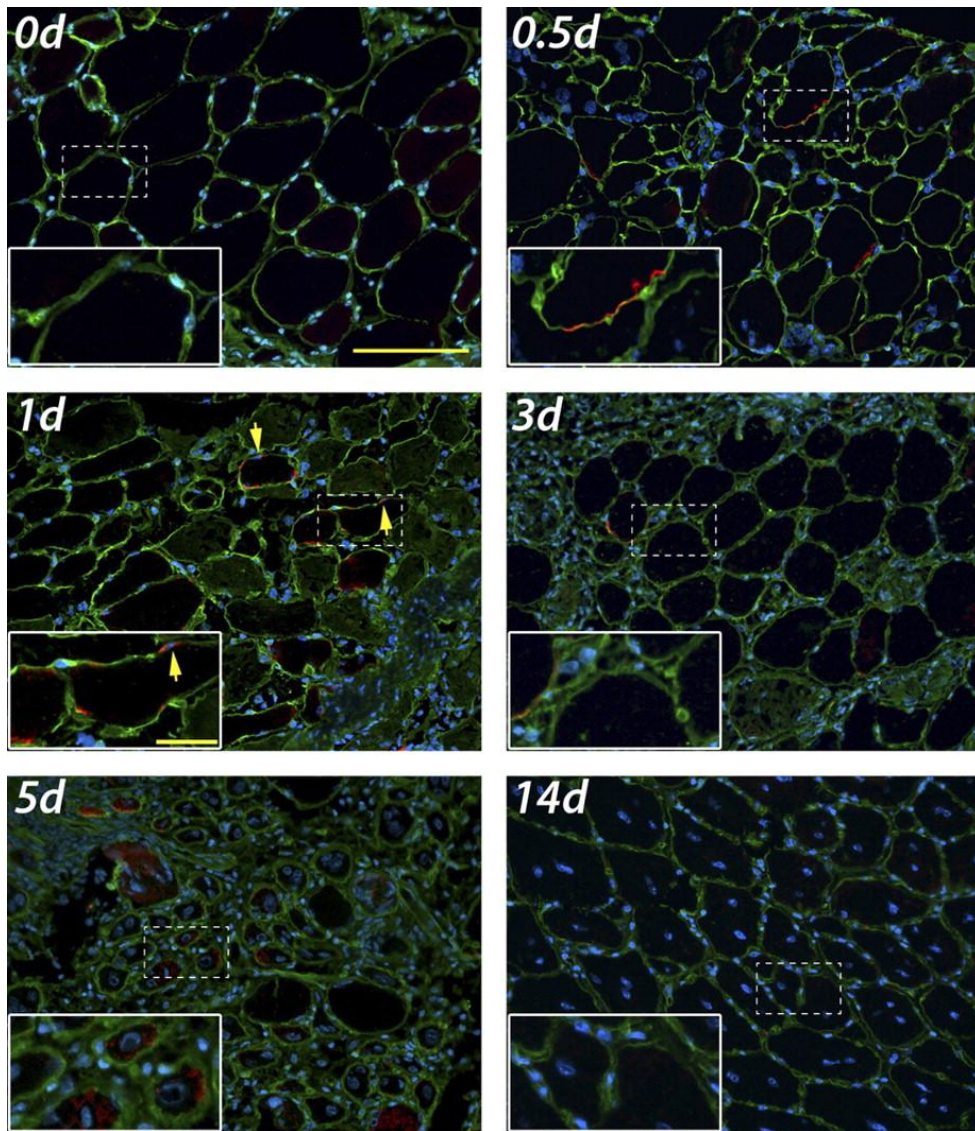


Figure 2.1. Immunohistochemical expression of Xin during skeletal muscle regeneration. Protein expression of Xin (red) within the mid-belly of the muscle is relatively low in the uninjured state (0 day; 0d). The expression increases within 12 hours (0.5d) of cardiotoxin-induced muscle injury. The expression of Xin is largely localized to the periphery of the muscle fibers (arrowheads). By 1 day (1d) post-injury, the expression of Xin is generally sub-laminar (laminin: green) and often at the periphery of the muscle fiber. There are also instances where this sub-laminar Xin expression is co-localized with nuclei (DAPI: blue) as noted by the yellow arrows. This expression pattern is characteristic of muscle satellite cells. By 3 days of regeneration (3d) there is a large inflammatory response evident as illustrated by the high level of interstitial nuclei. The expression of Xin is somewhat reduced when compared to the 1 day time point though

Xin expression is still observed at the periphery of muscle fibers. By 5 days post-injury (5d), the expression of Xin has increased and is observed primarily in newly regenerating muscle fibers (centrally-located nuclei; arrowheads). At 14 days of regeneration, Xin expression has returned to levels consistent with the pre-injury (0d) state. Bar = 100 μ m, which is consistent for all panels.

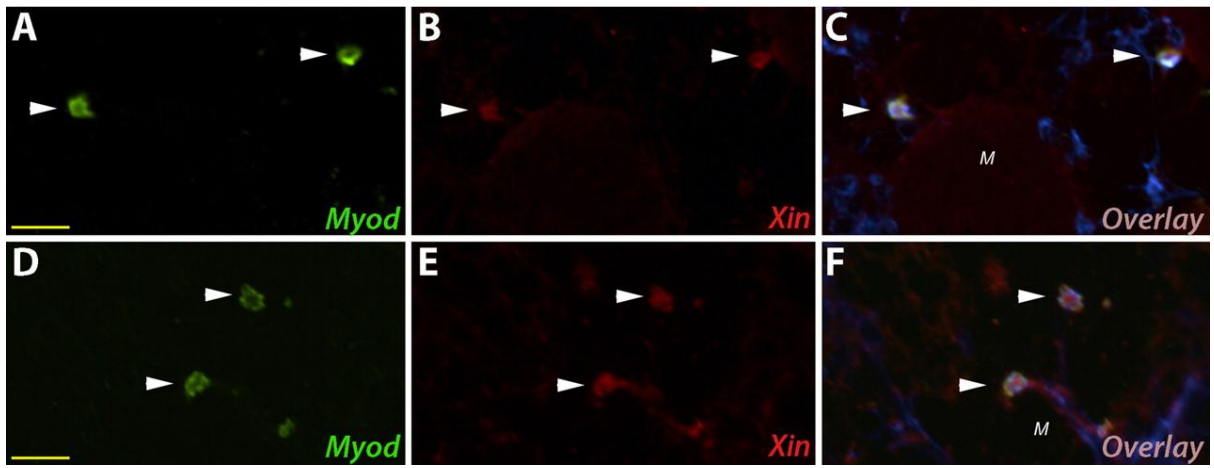


Figure 2.2. Co-localization of Xin and MyoD at 24 hours of skeletal muscle regeneration.

Panels A-C and D-F illustrate two examples of multiple MyoD positive areas (A and D) that co-localize with Xin expression (B and E) as illustrated in the overlay (C and F) which also includes DAPI to label all nuclei.

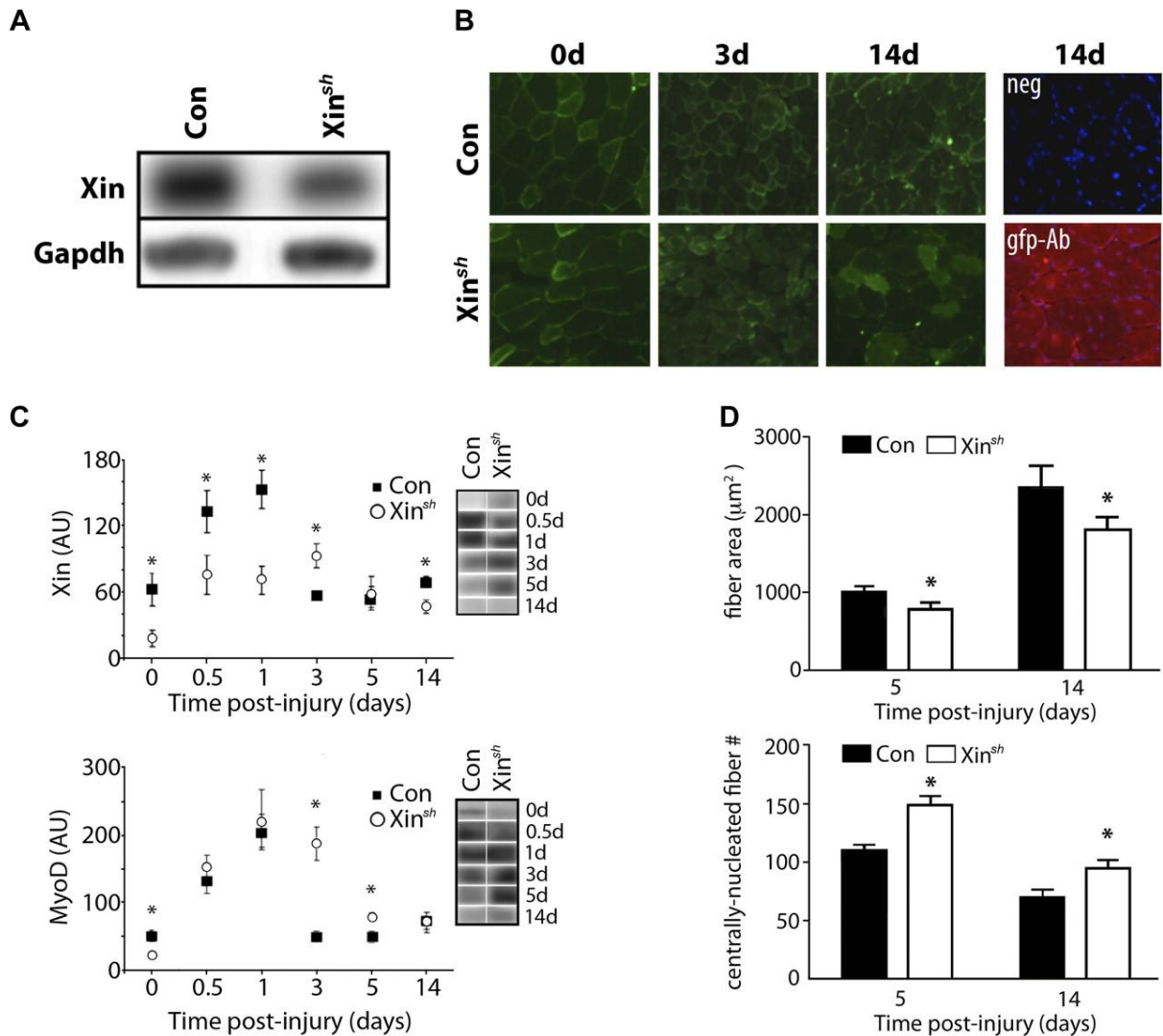


Figure 2.3. Xin-shRNA infection impairs skeletal muscle repair.

(A) Xin protein expression in GFP (Con) and Xin-shRNA (Xin^{-}) infected myoblasts demonstrated an approximately 60% decrease in endogenous Xin expression at 4 days post-infection. (B) Both Con and Xin^{-} vectors contained GFP, thus regions of infection could be identified. The right tibialis anterior (TA) was infected with Xin^{-} while the contralateral TA was infected with the Con adenovirus. Expression of GFP was evident throughout the experimental period for both vectors and the expression was confirmed in Xin^{-} muscle (14d) by using a GFP antibody and a Texas Red secondary. Negative control (Neg; absence of primary antibody) showed no signal. (C) Xin expression was detectable

at ~130 kDa at all time points suggesting that the Xin B isoform is the predominant isoform in skeletal muscle regeneration. The expression of Xin A isoform (~205 kDa) was faint/absent at all time points throughout (not shown). Xin- infection significantly reduced in endogenous Xin (open circles) at day 0 vs. Control (black squares). At 3 days of regeneration, expression of Xin returned to 0d levels while in the Xin- muscles, expression remained elevated, suggesting a continued pressure to promote the expression of Xin during regeneration. MyoD expression was robustly elevated at 24 hours and remained elevated at 3 day in Xin-shRNA, likely the result of delayed regeneration. Xin-shRNA and contralateral Control muscle samples (n=3-4/group) from each time point were run on the same gel to maintain temporal consistency. * denotes a significant difference between Con and Xin- samples at that given time point using a t-test. (D). The infection of skeletal muscle with Xin-shRNA resulted in a significant delay in muscle regeneration as noted by reduced regenerating myofiber areas at 5 and 14 days post-injury. The delayed regenerative capacity was further validated by quantifying the area of the muscle expressing embryonic myosin heavy chain (Myh3; lower panel) at 5 days post-injury.

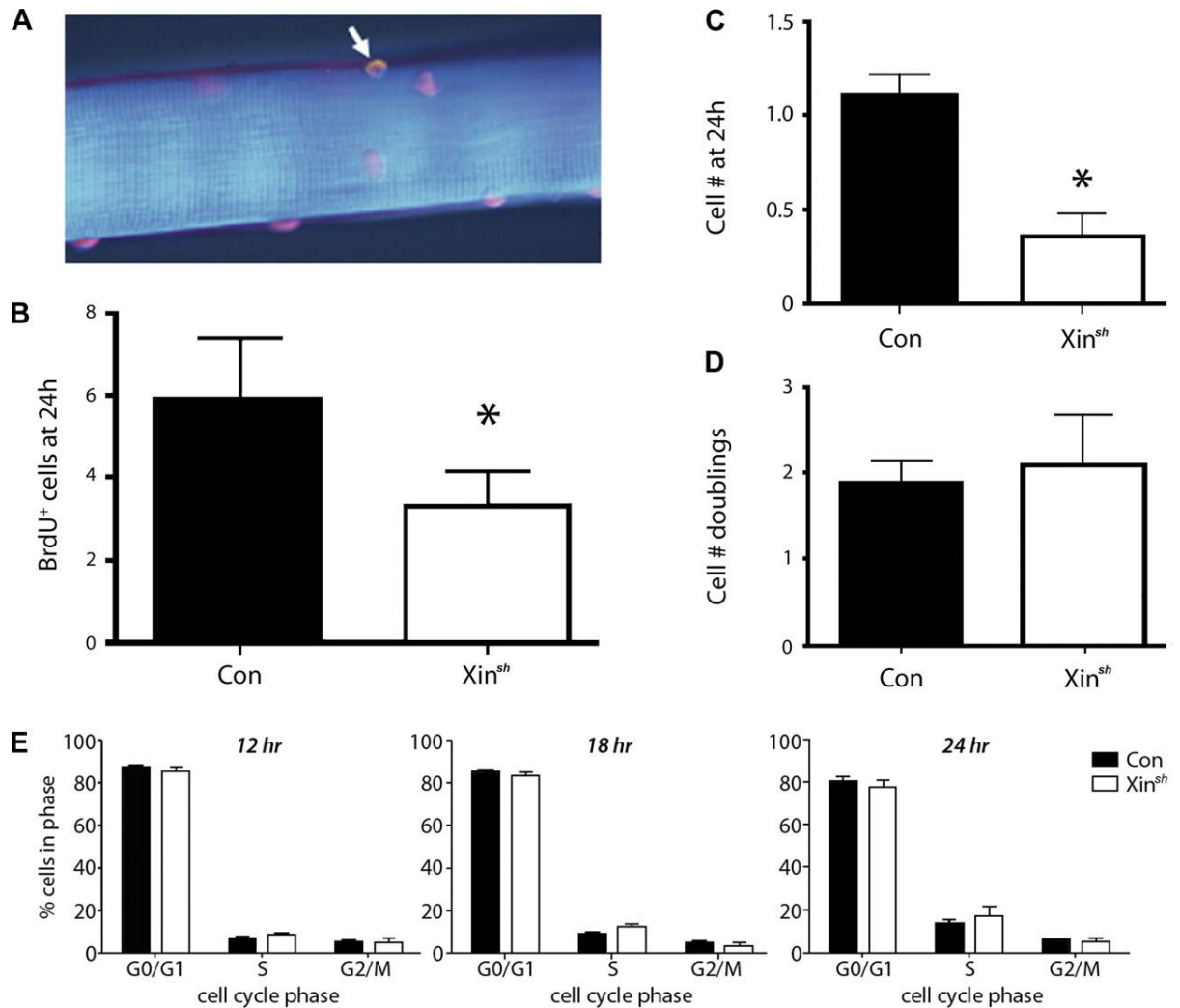


Figure 2.4. Repression of Xin impairs satellite cell activation.

Using floating single fibers infected with Xin-shRNA (Xin-) or Control (Con) adenoviruses and incubated with BrdU for 24 hours immediately following isolation, we were able to quantify the effect of Xin repression on the activation of satellite cells (20). (A) Illustrates a BrdU positive (arrow) nucleus on the periphery of an isolated muscle fiber. (B) A significant reduction in the number of BrdU positive satellite cells at 24 hours post-isolation was noted when Xin expression was repressed. (C) An alternative approach to assess satellite cell activation is to quantify the number of satellite cells that migrate from the isolated, adherent muscle fiber onto the cell culture plate. There was a significant reduction in the number of satellite cells that had migrated to the cell culture plate within the first 24 hours of isolation. (D) There was no difference between Xin- and

Con infected myoblasts in proliferative capacity. (E) To determine if Xin plays a role in cell cycle entry, Xin- and Con infected C2C12 myoblasts were arrested using a methylcellulose assay. Xin repression had no detectable effect on cell cycle re-entry.

Acknowledgements

The authors would like to thank the generous support of the Natural Sciences and Engineering Research Council of Canada (TJH) and the Canadian Institutes of Health Research (TJH).

References:

1. **Barash IA, Mathew L, Ryan AF, Chen J and Lieber RL.** Rapid muscle-specific gene expression changes after a single bout of eccentric contractions in the mouse. *Am.J.Physiol.Cell.Physiol.* 286: 2: C355-64, 2004.
2. **Beatham J, Gehmlich K, van der Ven PFM, Sarparanta J, Williams D, Underhill P, Geier C, Fürst DO, Udd B and Blanco G.** Constitutive upregulations of titin-based signalling proteins in KY deficient muscles. *Neuromuscul.Disord.* 16: 7: 437-445, 2006.
3. **Bischoff R.** Cell cycle commitment of rat muscle satellite cells. *J.Cell Biol.* 111: 1: 201-207, 1990.
4. **Bischoff R.** Regeneration of single skeletal muscle fibers in vitro. *Anat.Rec.* 182: 2: 215-235, 1975.
5. **Cooper RN, Tajbakhsh S, Mouly V, Cossu G, Buckingham M and Butler-Browne GS.** In vivo satellite cell activation via Myf5 and MyoD in regenerating mouse skeletal muscle. *J.Cell.Sci.* 112 (Pt 17): Pt 17: 2895-2901, 1999.
6. **Cornelison DD, Filla MS, Stanley HM, Rapraeger AC and Olwin BB.** Syndecan-3 and syndecan-4 specifically mark skeletal muscle satellite cells and are implicated in satellite cell maintenance and muscle regeneration. *Dev.Biol.* 239: 1: 79-94, 2001.

7. **Cornelison DD and Wold BJ.** Single-cell analysis of regulatory gene expression in quiescent and activated mouse skeletal muscle satellite cells. *Dev.Biol.* 191: 2: 270-283, 1997.
8. **Dhawan J, Lichtler AC, Rowe DW and Farmer SR.** Cell adhesion regulates pro-alpha 1(I) collagen mRNA stability and transcription in mouse fibroblasts. *J.Biol.Chem.* 266: 13: 8470-8475, 1991.
9. **Dlugosz AA, Antin PB, Nachmias VT and Holtzer H.** The relationship between stress fiber-like structures and nascent myofibrils in cultured cardiac myocytes. *J.Cell Biol.* 99: 6: 2268-2278, 1984.
10. **Hawke TJ, Atkinson DJ, Kanatous SB, Van der Ven PFM, Goetsch SC and Garry DJ.** Xin, an actin binding protein, is expressed within muscle satellite cells and newly regenerated skeletal muscle fibers. *Am.J.Physiol.Cell.Physiol.* 293: 5: C1636-44, 2007.
11. **Hawke TJ, Jiang N and Garry DJ.** Absence of p21CIP rescues myogenic progenitor cell proliferative and regenerative capacity in Foxk1 null mice. *J.Biol.Chem.* 278: 6: 4015-4020, 2003.
12. **Johnston AP, Baker J, Bellamy LM, McKay BR, De Lisio M and Parise G.** Regulation of muscle satellite cell activation and chemotaxis by angiotensin II. *PLoS One* 5: 12: e15212, 2010.

13. **Krause MP, Moradi J, Nissar AA, Riddell MC and Hawke TJ.** Inhibition of plasminogen activator inhibitor-1 restores skeletal muscle regeneration in untreated type 1 diabetic mice. *Diabetes* 60: 7: 1964-1972, 2011.
14. **Picciotto MR and Wickman K.** Using knockout and transgenic mice to study neurophysiology and behavior. *Physiol.Rev.* 78: 4: 1131-1163, 1998.
15. **Sambasivan R, Cheedipudi S, Pasupuleti N, Saleh A, Pavlath GK and Dhawan J.** The small chromatin-binding protein p8 coordinates the association of anti-proliferative and pro-myogenic proteins at the myogenin promoter. *J.Cell.Sci.* 122: Pt 19: 3481-3491, 2009.
16. **Sinn HW, Balsamo J, Lilien J and Lin JJ.** Localization of the novel Xin protein to the adherens junction complex in cardiac and skeletal muscle during development. *Dev.Dyn.* 225: 1: 1-13, 2002.
17. **van der Ven PFM, Ehler E, Vakeel P, Eulitz S, Schenk JA, Milting H, Micheel B and Fürst DO.** Unusual splicing events result in distinct Xin isoforms that associate differentially with filamin c and Mena/VASP. *Exp.Cell Res.* 312: 11: 2154-2167, 2006.
18. **Volonte D, Liu Y and Galbiati F.** The modulation of caveolin-1 expression controls satellite cell activation during muscle repair. *FASEB J.* 19: 2: 237-239, 2005.

19. **Wang DZ, Reiter RS, Lin JL, Wang Q, Williams HS, Krob SL, Schultheiss TM, Evans S and Lin JJ.** Requirement of a novel gene, Xin, in cardiac morphogenesis. *Development* 126: 6: 1281-1294, 1999.
20. **Wozniak AC, Kong J, Bock E, Pilipowicz O and Anderson JE.** Signaling satellite-cell activation in skeletal muscle: markers, models, stretch, and potential alternate pathways. *Muscle Nerve* 31: 3: 283-300, 2005.

Chapter 3: PREFACE

Significance to thesis

The primary goal of this study was to further understand the contribution of Xin to skeletal muscle regeneration, using a Xin-deficient (Xin^{-/-}) mouse model. The previous study showed that Xin-shRNA infected muscle regeneration was attenuated, and satellite cell activation was reduced when endogenous Xin is reduced by ~60%. Xin-deficient mice do not express any isoform of Xin, and appear to undergo normal development except for a mild cardiac phenotype. This novelty of this study lies in the fact that the skeletal muscle of these mice had not been examined. Therefore, the first aim of this study was to characterize skeletal muscle morphology in the non-injured Xin^{-/-} mouse to determine if any signs of myopathy are present. Since Xin has been implicated in the regenerative process, the second aim was to assess the timecourse of Xin^{-/-} skeletal muscle repair compared to wild type animals. If Xin^{-/-} skeletal muscle regeneration was impaired as hypothesized, aim three was to determine any alterations in Xin^{-/-} satellite cell function that would have affected muscle repair. Therefore using a model that completely lacks Xin will advance the current knowledge of the role of Xin within skeletal muscle repair and satellite cell function.

Contribution of Authors

Aliyah A. Nissar contributed to the design of the studies, performed the experiments and data collection, performed microscope and statistical analysis on the data, and wrote the initial draft of the manuscript.

Peter F. M. van der Ven and Dieter O. Fürst contributed to the design of the study, and provided Xin-deficient mice.

Thomas J. Hawke designed the study, performed and assisted in experiments, edited the manuscript and funded the studies.

Skeletal muscle and satellite cell characterization of Xin-deficient mice

Aliyah A. Nissar¹, Peter F. M. van der Ven², Dieter O. Fürst², Thomas J. Hawke¹

¹Pathology and Molecular Medicine, McMaster University. Hamilton ON. Canada

²Institute for Cell Biology, University of Bonn, Bonn, Germany

Running title: Xin^{-/-} mice skeletal muscle

Keywords: muscle regeneration, satellite cells, Xin, cardiotoxin

Word count: 5553

Correspondence and request for materials should be addressed to:

Thomas J. Hawke, Ph.D.

Pathology & Molecular Medicine, McMaster University,

1200 Main St. W., Hamilton ON. Canada, L8N 3Z5.

Phone: 905-525-9140 ext 22372

Email: hawke@mcmaster.ca

Abstract

The ability for terminally differentiated skeletal muscle to respond to injury and physiological stressors is due, in part to its resident stem cell population, termed satellite cells (SCs). We have previously identified Xin, a striated-muscle specific, cytoskeletal adapter protein, to be highly upregulated early after muscle injury and localized to the SC population. In this study, we used novel Xin-deficient (Xin^{-/-}) mice to determine the role of Xin in skeletal muscle repair and satellite cell regulation. Xin-deficient mice display significant differences in embryonic myosin heavy chain expression and muscle fiber size compared to wildtype (WT) mice up to 35 days post-injury, indicative of a significant impairment in muscle regeneration. While there was no significant differences in Pax7⁺ SC number between Xin^{-/-} and WT in resting muscle, Xin^{-/-} mice displayed increased activation capacity assessed using BrdU incorporation, since more Xin^{-/-} SCs were activated at rest. However, compensation for the lack of Xin which resulted in SC hyperactivation did not translate to SC proliferative capacity. Xin-deficient SCs displayed a significant reduction in proliferation, thereby explaining impaired muscle regeneration in this mouse model of myopathy. This data demonstrates the importance of Xin in SC function and therefore skeletal muscle repair.

Introduction

The ability for skeletal muscle to adapt to physiological stressors and regenerate following injury is largely attributed to its satellite (stem) cell population. Satellite cells leave quiescence and become activated in response to myotrauma, when extensive remodelling and growth of their cytoskeleton occurs. They then begin to proliferate, at which point they are termed myoblasts. Myoblasts differentiate to form new myofibers or repair damaged muscle fibers. However, the mechanisms that govern these processes are relatively unknown. Xin, a striated-muscle specific cytoskeletal protein was found to be upregulated within damaged mouse skeletal muscle during early phases in the regenerative process, and also localized to satellite cells (7, 8, 12). Furthermore, Xin expression has been observed in newly regenerating muscle fibers, as defined by their centrally located nucleus (7, 12). The role of Xin within satellite cells and muscle regeneration has yet to be fully understood.

Xin is the protein encoded by the human gene Xin-repeat protein 1' (XIRP1) (previously referred to as 'Cardiomyopathy associated 1' or CMYA1) which consist of two exons. Splicing of these exons leads to three isoforms of Xin: XinA, XinB and XinC. In uninjured adult skeletal muscle, Xin mRNA presence is negligible and subsequent protein expression is primarily detected at the myotendinous junction (MTJ) (15). However, in response to muscle damage, Xin mRNA is elevated with a peak in expression 12 hrs post-injury (1, 2, 7). This translates to Xin protein expression at the myofiber periphery and localized to satellite cells 12-24 hrs post-injury, and within regenerating fibers after 5 days of muscle repair (12). When endogenous Xin expression was reduced in mouse

skeletal muscle through intramuscular injections of a Xin-shRNA adenovirus, a delay in muscle regeneration and reduced capacity for SC activation were observed (12). PCR analysis demonstrated the introduction of Xin-shRNA resulted in a 50% decrease in Xin mRNA, confirmed by Western analysis, which showed a 60% reduction in endogenous Xin (7).

The purpose of the present study was to further understand the role of Xin in muscle regeneration and satellite cell function using Xin-deficient (Xin^{-/-}) mice, which lacks all Xin isoforms. These mice undergo normal development and only exhibit a mild cardiac phenotype (13), however their ability for skeletal muscle regeneration has not been explored.

Our results indicate Xin^{-/-} mice have a decrease in glycolytic (type IIB) fibers, which is common in myopathic muscle (11), and a subsequent increase in IIA fiber size. The lack of Xin also resulted in impaired muscle regeneration following cardiotoxin injury, demonstrated by fiber area and Myh3 (embryonic myosin heavy chain) expression. Results suggest impaired regeneration is attributed to alterations in satellite cell function, since Xin^{-/-} satellite cells are hyperactivated, but have reduced proliferative capacity. Overall, this study highlights the importance of Xin in satellite cell function, as the compensation for the elimination of Xin causing hyperactivation, likely resulted in decreased satellite cell proliferation, thereby causing impaired muscle regeneration.

Materials/ Methods

Animals

Xin^{-/-} mice were developed by replacing the Xin protein coding sequence with a cassette containing an internal ribosomal entry site that drives lacZ and neomycin gene expression, in a C57Bl/6 background as previously described (13). After receiving these mice from Dr. Dieter Fürst (University of Bonn, Germany), they were genotyped to ensure complete ablation of Xin using Xin and neomycin primer pairs (Xin fw 3'-GAGTTCAAAGCAATGCAGTGAGG-5'; Xin rev 3'-TTCAAACAGATGTCGCTGATGCTG-5'; Neo fw 3'-CGTGTTCGGCTGTCAGCGCAGG-5'; Neo rev 3'-CAACGCTATGTCCTGATAGCGGTCC-5')

Male C57Bl/6 Xin^{-/-} mice and C57Bl/6 wildtype [WT; Jackson Laboratories (Bar Harbor, ME)] mice (3-5 mo of age) were used for these studies. Both murine strains were provided with enrichment material, standard breeder chow and water ad libitum. Animal housing conditions were maintained at 21°C, 50% humidity, and 12 h/12 h light-dark cycle. All experimental protocols were approved by the McMaster University Committee on Animal Care and performed in accordance with the Canadian Council Animal Care guidelines.

Skeletal Muscle Injury

The left tibialis anterior (TA) muscle of *Xin*^{-/-} and WT mice was injured using a 100- μ l intramuscular injection of 10 μ M cardiotoxin (CTX; Latoxan, Valence, France), resulting in almost complete muscle degeneration (7). To characterize the process of skeletal muscle regeneration of *Xin*^{-/-} mice compared to WT, the TA muscles were harvested at 3, 5, 10, 14 and 35 days postinjury (*n*=5: *Xin*^{-/-} ; WT). The right, uninjured TA muscle was also harvested as an internal control.

Tissue Collection

Animals were euthanized by cervical dislocation after CO₂ inhalation. The TA muscles from *Xin*^{-/-} and WT mice were dissected, coated with tissue-mounting media, and frozen in isopentane cooled by liquid nitrogen for histochemical and immunofluorescent analyses. Uninjured EDL and peroneus longus muscles from both animal strains were harvested to isolate single muscle fibers. Lastly, uninjured hind-limb TA, GPS, quadriceps, and hamstring muscles of *Xin*^{-/-} and WT mice were harvested to isolate satellite cells, also referred to as primary myoblasts.

Single Muscle Fiber Isolations

Single muscle fibers were collected from *Xin*^{-/-} and WT EDL and peroneus longus muscles, as previously described (9). Briefly, muscles were dissected and digested in 0.2% (w/v) type 1 collagenase solution, in a shaking incubator for 90 minutes at 37°C. Single fibers were isolated by titrating muscle bundles in low glucose Dulbecco's

modified Eagle's medium (DMEM; invitrogen), and incubated in culture dishes containing plating media (10% normal horse serum, 0.5% chick embryo extract, in DMEM) for 24hr SC activation analysis. Single fibers were also fixed immediately after isolation in 4% paraformaldehyde (PFA) for 0 hr SC activation and Pax7 analysis.

Satellite Cell Activation Analyses

The activation of satellite cells was assessed by the incorporation of BrdU into cells that entered the cell cycle, and therefore analyzed as the number of BrdU+ cells satellite cells per single fiber surface area. Single fiber surface area was calculated assuming a cylindrical shape, by measuring the length of the fiber, and the average width at multiple points. To determine the capacity for satellite cells to become activated, newly isolated Xin^{-/-} and WT single fibers were incubated in plating media containing 10 μ M 5-bromo-2-deoxyuridine (BrdU; Sigma 858811) for 24 hours. After which, fibers were fixed in 4% PFA and incubated in BrdU antibody (Sigma B2531) diluted 1:25 overnight at 4°C. A biotin-streptavidin (Vector Labs) detection system was used to visualize BrdU+ satellite cells, as previously described (12, 16). Briefly, after endogenous streptavidin and biotin was blocked, fibers were incubated in secondary anti-mouse biotin (2 μ g/ml; 1:250) for 30 minutes. After washing in PBS, fibers were incubated in streptavidin anti-biotin Dylight 488 (1:350) with propidium iodide (200 μ g/ml; 1:5; used to stain all nuclei) for 30 min. A total of 30 fibers from an $n=4$ animals were analyzed from both Xin^{-/-} and WT mice.

To determine the number of activated satellite cells in the resting muscle (0 hr), Xin^{-/-} and WT mice received an i.p injection of BrdU (10.5 mg), and were harvested 20 hrs after administration. Single fibers were isolated, fixed right away in 4% PFA, and BrdU⁺ cells were stained as described above. A total of 10 fibers were analyzed from both animal strains.

Satellite Cell Proliferation Analysis- Primary Myoblasts

To determine the proliferative capacity of Xin^{-/-} vs. WT myoblasts, hind-limb skeletal muscles, including TA, GPS, quadriceps and hamstring were harvested ($n=3$ from each group). Tendons, large arteries and nerves were removed from the muscles to decrease contamination of other cell types. Muscles were lightly chopped and incubated in type III collagenase (0.2% w/v in high-glucose DMEM) for 45 min at 37°C. The collagenase solution was discarded, and the muscles were incubated in a dispase solution (BD biosciences) in high-glucose DMEM (16 c.u./ml DMEM) for 30 mins at 37°C. After which, a sterile 70- μ m filter was used to eliminate debris and remaining muscle bundles. The cells were washed in PBS, resuspended in growth media, and pre-plated in a 60 mm plate to remove contaminants, and increase purity of myoblast yield. The primary myoblasts were then plated at a known concentration in a 6-well plate. The myoblasts were allowed to settle before they were counted and the growth media was renewed. After having proliferated for 18 hrs, the myoblasts were recounted to determine the percent increase.

Histochemical and Immunofluorescent Analyses

Hematoxylin and eosin stain

Hematoxylin and eosin (H&E) stains were performed by transversely cutting TA muscles into 8 μm cross-sections, which were adhered to charged glass slides. Xin^{-/-} and WT TA fiber area were analyzed in the uninjured muscle, and after 14 and 35 days of regeneration. Injured fibers were selected by the presence of centrally located nuclei. Fiber areas were analyzed for 100 fibers throughout each muscle section (n=5 from each group).

Immunofluorescent staining

Xin^{-/-} and WT type IIA and IIB fiber size and percentage were determined by fixing 8 μm uninjured TA cross sections in cold 2% PFA, incubating in block (10% normal goat serum and 1.5% bovine serum albumin) for 30 mins at room temperature (RT), followed by mouse IgG block (Vector, BMK2202) for 1 hr at RT. Sections were then incubated in either IIA or IIB antibody (Hybridoma Bank; 2F7; 10F5 respectively) at a 1:1 concentration in PBS overnight at 4°C. To visualize IIA/IIB staining, sections were incubated in Alexa 594 anti-mouse secondary antibody, for 90 min (1:1000) at RT. To accurately measure fiber area, sections were blocked, and co-stained with Collagen IV antibody (Abcam; ab6568) diluted 1:250 for 1 hr at RT, allowing the detection of muscle fiber membranes. This was visualized using Alexa 488 anti-rabbit (1:1000) for 1hr at RT. A drop of 1:10,000 4,6-diamidino-2-phenylindole (DAPI) was applied briefly to identify nuclei. Approximately 100 type IIA and IIB fiber areas were in each muscle section, and

fiber type percentages were calculated by counting the number of each fiber type as a percent of total number of muscle fibers ($n=3$ from each group).

Embryonic myosin heavy chain (Myh3) expression was analyzed in *Xin*^{-/-} and WT TA sections (8 μm), 3; 5; 10; and 14 days following cardiotoxin injury, as described previously (12). Briefly, sections were fixed in 2% PFA, blocked, and incubated in undiluted Myh3 antibody (Hybridoma Bank; F1.652) at 4°C overnight. To visualize muscle fibers which express Myh3, Alexa 488 anti-mouse antibody (1:1000) was applied to the sections for 1 hr at RT. Embryonic myosin heavy chain positive area was analyzed as a percent of total injured area in each muscle cross-section ($n=5$ from each group, for each time point).

The total number of satellite cells (activated and quiescent) in *Xin*^{-/-} and WT muscle was determined by Pax7 (14) analysis of both muscle cross-sections and single fibers. Transverse 6 μm uninjured TA sections ($n=3$ from each group), and isolated single fibers (20 fibers from each group) were fixed immediately in 2% PFA. After washing with PBS, 1% triton in PBS was applied for 30 min at RT. The sections and single fibers were then blocked (1.5% normal goat serum, 1.5% normal horse serum) for 30 min at RT, and Pax7 antibody (Hybridoma Bank) diluted 1:1 was applied overnight at 4°C. After application of streptavidin-biotin block, sections and fibers were incubated in secondary anti-mouse biotin (2 $\mu\text{g}/\text{ml}$; 1:250) for 30 minutes, then streptavidin anti-biotin dylight 594 (1:250) for 30 mins. Single fibers were briefly incubated in DAPI (1:10000) to identify nuclei. Muscle sections were further incubated in laminin (abcam; 14055) diluted 1:250 for 1 hr at RT, to identify Pax7⁺ cells that were under the fiber basal

lamina. This was visualized by 30 min incubation in Alexa 488 anti-chick antibody (1:250), followed by DAPI. The number of Pax7⁺ satellite cells in the muscle cross-section was analyzed as a percent of total nuclei, whereas the number of Pax7⁺ cells per single fiber was assessed by fiber surface area.

Xin^{-/-} and WT satellite cell proliferation was further assessed by immunofluorescent staining of TA muscle 3 days post-injury for the myogenic regulatory factor, MyoD, which is a marker of proliferating myoblasts (4). Transverse TA sections (6 μm) were fixed, blocked (10% normal goat serum, 1.5% bovine serum albumin, 0.3% triton), and incubated in MyoD antibody (Abcam; ab64159) diluted 1:100 and incubated overnight at 4°C. Sections were subsequently incubated in Alexa 488 anti-rabbit antibody (1:250) for 1 hr at RT, followed by DAPI. MyoD expression was assessed as a percentage of total injured area of each muscle section (*n*=5 for both groups).

Image Analysis

A Nikon 90i eclipse upright microscope was used to capture x20 images of stained muscle sections and single fibers. Nikon elements software was used to analyze images. Fiber areas and fiber type percentage were determined by manually outlining and counting fibers. Expression of Myh3, MyoD and Pax7 in muscle sections were analyzed using threshold detection for positive areas above background. Satellite cells positive for BrdU or Pax7 on single fibers were manually counted, and the fiber surface area was measured.

Statistical Analysis

Student's two-tailed t-tests were used to determine significant differences ($P < 0.05$) in data obtained from $Xin^{-/-}$ and WT muscles. A 2-way ANOVA was used to test for significant differences ($P < 0.05$) in each fiber size category between the two groups. Data are presented as means \pm SE.

Results

Xin deficiency results in altered skeletal muscle morphology

To elucidate the importance of Xin in skeletal muscle, we utilized Xin-deficient (Xin^{-/-}) mice which lacks all three Xin isoforms. Although these mice develop normally and display no overt phenotype, analysis of Xin^{-/-} skeletal muscle revealed morphometrical differences compared to wildtype (WT) age-matched controls. H&E stains were used to determine fiber area, and immunofluorescent stains to decipher between type IIA/IIB fiber area, and type IIA/IIB fiber percentage. Although there was no significant difference between the mean fiber area of Xin^{-/-} and WT muscle (Xin^{-/-}: 1949 ± 199 $n=3$ vs. WT: 2244 ± 96 $n=3$; $P=0.23$), Fig. 3.1A displays a trend towards more small fibers in Xin^{-/-} muscle, with significantly more fibers on the low end of the size spectrum, between 1200 and 1600 μm^2 . Type IIA fibers were found to be slightly, but significantly larger in Xin^{-/-} mice (Fig. 3.1B; Xin^{-/-}: 1690 ± 29 μm^2 $n=3$ vs. WT: 1527 ± 29 μm^2 $n=3$; $P=0.017$), whereas there was no significant difference in type IIB fiber size between the groups (Fig. 3.1C; Xin^{-/-}: 4761 ± 247 μm^2 $n=3$ vs. WT: 5157 ± 318 μm^2 $n=3$; $P=0.38$). There was also no difference in the number of type IIA fibers expressed as a percent of the total number of fibers in the muscle section between the groups (Fig. 3.1D; Xin^{-/-}: 3.14 ± 0.70 μm^2 $n=3$ vs. WT: 3.89 ± 0.44 μm^2 $n=3$; $P=0.42$). However, Xin^{-/-} IIB fiber type percentage was significantly lower in the TA muscle compared to WT (Fig. 3.1E; Xin^{-/-}: $57.04 \pm 1.29\%$ $n=3$ vs. WT: $66.02 \pm 1.87\%$ $n=3$; $P=0.017$).

Skeletal muscle regeneration following cardiotoxin injury is impaired in *Xin*^{-/-} mice

The complete lack of *Xin* resulted in impaired muscle regeneration following injury, assessed by *Myh3* expression and fiber sizes throughout the repair process (Figure 3.2). *Xin*^{-/-} mice and age-matched WT sustained a left leg cardiotoxin injury, and TA muscles were harvested at 3, 5, 10, 14, and 35 days post-injury. Embryonic myosin heavy chain is expressed in newly formed, small muscle fibers before they enlarge and switch to mature forms of myosin, and was analyzed as a percent of total injured area. *Xin*^{-/-} mice display a different *Myh3* expression profile following injury compared to WT. At 3 days post-injury, there is a trend towards decreased *Myh3* expression in *Xin*^{-/-} regenerating muscle compared to WT (Fig. 3.2A; *Xin*^{-/-}: $0.142 \pm 0.050\%$ $n=5$ vs. WT: $0.422 \pm 0.130\%$ $n=5$; $P=0.08$). This suggests a delay in *Xin*^{-/-} muscle to initiate the muscle repair process, since there is less muscle fiber formation occurring. After 5 days of muscle repair, there is significantly more *Myh3* expression in *Xin*^{-/-} muscle (Fig. 3.2A; *Xin*^{-/-}: $25.04 \pm 2.65\%$ $n=5$ vs. WT: $16.32 \pm 1.57\%$ $n=5$; $P=0.022$). This data indicates that while WT fibers are maturing and no longer expressing *Myh3*, *Xin*^{-/-} fibers are delayed in this process. Results continue to show this expression pattern throughout the remaining timeline of regeneration. There is a trend towards increased *Myh3* expression in *Xin*^{-/-} muscle at 10 days post-injury (Fig. 3.2A; *Xin*^{-/-}: $2.90 \pm 0.75\%$ $n=5$ vs. WT: $1.64 \pm 0.51\%$ $n=5$; $P=0.20$). By 14 days of regeneration, unlike *Xin*^{-/-} muscle, there is almost no *Myh3* expression in WT (Fig. 3.2A; *Xin*^{-/-}: $0.84 \pm 0.19\%$ $n=5$ vs. WT: $0.05 \pm 0.02\%$ $n=5$; $P=0.003$; Fig. 3.2C), which is indicative of impaired regeneration of *Xin*^{-/-} skeletal muscle.

This data is confirmed by the H&E analysis of regenerating myofiber size, identified by centrally located nuclei in TA muscle cross-sections. Figure 3.2B and 3.2C displays significantly smaller *Xin*^{-/-} average fiber area compared to WT, 14 and 35 days post-injury (14d; *Xin*^{-/-}: $1307 \pm 99 \mu\text{m}^2$ $n=5$ vs. WT: $2359 \pm 148 \mu\text{m}^2$ $n=5$; $P= 0.0004$; 35d; *Xin*^{-/-}: $1280 \pm 130 \mu\text{m}^2$ $n=5$ vs. WT: $2897 \pm 360 \mu\text{m}^2$ $n=4$; $P= 0.0024$). Importantly, after 35 days of muscle repair, *Xin*^{-/-} fibers did not grow to pre-injury size, whereas WT fibers were larger than their initial size. This confirms the diagnosis of impaired regeneration in *Xin*^{-/-} mice following injury, therefore *Xin* is important in the muscle repair process.

Elimination of *Xin* results in hyperactivated satellite cells but reduced proliferative capacity

Satellite cells are a primary contributor to skeletal muscle regeneration, and therefore it was important to determine if alterations in SC function exists in *Xin*^{-/-} mice. Two methods were used to identify quiescent satellite cell number at rest: TA muscle cross-sections, and EDL/peroneus longus single fibers were immunofluorescently stained for Pax7, a known satellite cell marker. Results indicate that there is no significant difference in the number of quiescent satellite cells in muscle sections between the groups (Fig. 3.3A; *Xin*^{-/-}: $1.74 \pm 0.15\%$ $n=3$ vs. WT: $1.91 \pm 0.15\%$ $n=3$; $P= 0.45$), where Pax7⁺ SCs were determined to be co-localized with nuclei marker DAPI, and under laminin, and was calculated as a percent of total nuclei. Also, single fiber analysis of 20 fibers derived from 2 mice in each group showed a slight increase in average *Xin*^{-/-} Pax7⁺ SCs compared to WT, expressed as the number of Pax7⁺ cells per μm^2 of fiber surface area

(multiplied by 1000) (Fig. 3.3B; $Xin^{-/-}$: 0.0149 ± 0.0013 vs. WT: 0.0119 ± 0.0011 ; $P=0.08$).

Since no significant difference in satellite cell number was observed, we looked for alterations in satellite cell activation that may account for impaired regeneration of $Xin^{-/-}$ muscle. Contrary to our hypothesis, after allowing 24 hours of BrdU incorporation in activated SCs of isolated single fibers in vitro, immunofluorescent staining indicated a significant increase in $Xin^{-/-}$ BrdU+ SCs compared to WT (Fig. 3.3C; $Xin^{-/-}$: 0.0280 ± 0.0007 $n=4$ vs. WT: 0.0191 ± 0.0003 $n=4$; $P<0.0001$), assessed by colocalization of BrdU+ cells with nuclei labelled with propidium iodide, and calculated as the number of BrdU+ cells per μm^2 of fiber surface area (multiplied by 1000). To contribute to the understanding of the role of Xin in satellite cells, it was important to identify if $Xin^{-/-}$ SCs are constitutively active at rest (Fig. 3.3D; 0 hr), when theoretically few SCs should be active. Therefore, BrdU was injected in $Xin^{-/-}$ and WT uninjured muscle, and allowed to incorporate into any cells actively dividing for 20 hours before 10 single fibers derived from 2 mice in each group were harvested and fixed. Results indicate on average, more satellite cells are activated/dividing in the resting $Xin^{-/-}$ animal compared to WT, expressed per μm^2 of fiber surface area (multiplied by 1000) (Fig. 3.3E; Fig. 3.3D; $Xin^{-/-}$: 0.0117 ± 0.0024 vs. WT: 0.00530 ± 0.0011 ; $P=0.038$). Therefore, since there is no significant difference in the number of SCs at rest between groups, it can be concluded based on BrdU incorporation at rest that $Xin^{-/-}$ SCs are hyperactivated.

However, these results did not explain why there is delayed regeneration in $Xin^{-/-}$ mice. Therefore, myoblast proliferation was analyzed using two methods: primary myoblast cell

counts, and MyoD expression in 3 day injured muscle. Primary myoblasts were isolated from both animal strains and analyzed as a percent increase in myoblast number after 18 hours of proliferation. Results indicate an approximately 50% reduction in *Xin*^{-/-} myoblast proliferation compared to WT (Fig. 3.4A; *Xin*^{-/-}: $51.0 \pm 6.1\%$ $n=3$ vs WT: $103.6 \pm 7.9\%$ $n=3$; $P=0.0062$). To confirm these results, 3 day post-injury muscle sections were immunofluorescently stained for MyoD, the myogenic regulatory factor that is a marker of proliferating myoblasts. Results indicate that there is a trend for less MyoD⁺ area, assessed by co-localization with nuclei marker DAPI, in *Xin*^{-/-} injured muscle sections compared to WT (Fig. 3.4C; Fig. 3.4B; *Xin*^{-/-}: $0.39 \pm 0.13\%$ $n=5$ vs. WT: $1.01 \pm 0.30\%$ $n=5$; $P=0.1$). Taken together, these data indicate *Xin*^{-/-} satellite cells are compensating for the lack of *Xin*, causing satellite cells to be hyperactivated. However, this compensatory mechanism proves to be detrimental to satellite cell proliferation, resulting in impaired muscle regeneration.

Discussion

Our previous studies demonstrated Xin mRNA is upregulated early in the regenerative process (7). Xin protein is co-localized with markers of satellite cells, expressed at the periphery of muscle fibers (consistent with SCs) following injury, and within newly forming fibers during muscle regeneration. The reduction of Xin in vivo through Xin shRNA resulted in attenuated muscle regeneration, likely caused by reduced satellite cell activation (12). However, in our current study we utilize a Xin-deficient mouse model to further determine the role of Xin in skeletal muscle morphology and regeneration, and satellite cell function. Results indicate differences in myofiber size and type, impaired regeneration even after 35 days of repair, and altered satellite cell function of Xin^{-/-} mice. Therefore our findings confirm the role of Xin in the muscle regenerative process, including satellite cell function.

The importance of Xin in skeletal muscle is fundamentally recognized by alterations in muscle morphology at rest when Xin is eliminated. Xin-deficient muscle shows characteristics of myopathy, since a reduction in glycolytic (type IIB) fibers is observed (11), resulting in a slight increase in type IIA fiber size to compensate. Although there is no difference in average fiber size, there is a trend for smaller fibers in Xin^{-/-} muscle. Since type IIA fibers are significantly larger, and there is no difference in the number of type IIA fibers, the increase in smaller fibers may be attributed to type IID fibers.

Skeletal muscle repair following injury is characterized by inflammation and degeneration of damaged myofibers, and activation of quiescent satellite cells which

proliferate and differentiate to regenerate muscle fibers (4, 4, 8, 10). This study shows when Xin is eliminated, skeletal muscle regeneration is not only delayed, but also impaired, determined by analyzing muscle 3 to 35 days after cardiotoxin injury. Specifically, the formation of new fibers is delayed in Xin^{-/-} muscle, likely the result of reduced proliferating myoblasts 3 days post-injury. Xin^{-/-} muscle regenerates slower overall, since Myh3 expression exists at 14 days post-injury, where expression in WT muscle is virtually absent. This indicates impairment in Xin^{-/-} myofibers to mature, and ultimately obtain pre-injury fiber size. At 35 days post-injury, unlike Xin^{-/-} myofibers, WT fibers have undergone hypertrophy, and surpassed pre-injury size. This result highlights a possible role for Xin in myofibril assembly, and therefore the lack of Xin results in reduced growth/hypertrophy. Myofibrillar assembly involves the organization of individual proteins into thick filaments, thin filaments and Z-lines. Studies have indicated the requirement of proteins which scaffold the assembly of actin and α -actinin into premyofibril structures during the first steps of assembly. An example of a scaffold protein, N-RAP, is a LIM domain nebulin-repeat protein (6). Interestingly, Xin-repeats have been shown to bind to F-actin in a similar manner as nebulin-repeats (5). Therefore, this hypothesis is feasible, since Xin is observed within regenerating fibers around 5 days post-injury (12), and therefore may play a role in assisting in myofiber growth at this time point.

Another mediator of impaired regeneration in Xin^{-/-} muscle may be attributed to alterations in satellite cell function. Previous studies showed decreased SC activation when Xin was reduced using shRNA, however no affect on proliferation (12). This study

supports the findings that Xin is important in SC activation, as Xin^{-/-} mice appear to be compensating for the complete elimination of Xin by hyperactivating satellite cells at rest. When satellite cells become activated, cytoskeletal remodelling occurs to allow for increased cell size (3). Therefore, since Xin is an actin-binding protein, a possible role within the activation of satellite cells may be to contribute to cellular hypertrophy. However, the mechanism compensating for the lack of Xin in SC activation, appears to be detrimental to SC proliferation, resulting in decreased myoblasts, and therefore delayed regeneration. Based on previous studies, it is not likely that Xin plays a direct role in SC proliferation, since no affect on proliferative capacity was displayed in Xin shRNA muscle, where compensatory proteins were negligible (12).

In conclusion, these data demonstrates the importance of Xin in satellite cell activation, and muscle regeneration, where Xin may be crucial in cellular hypertrophy in both instances. Future studies will aim to elucidate the role Xin plays in satellite cell activation by determining Xin protein interaction partners within SCs.

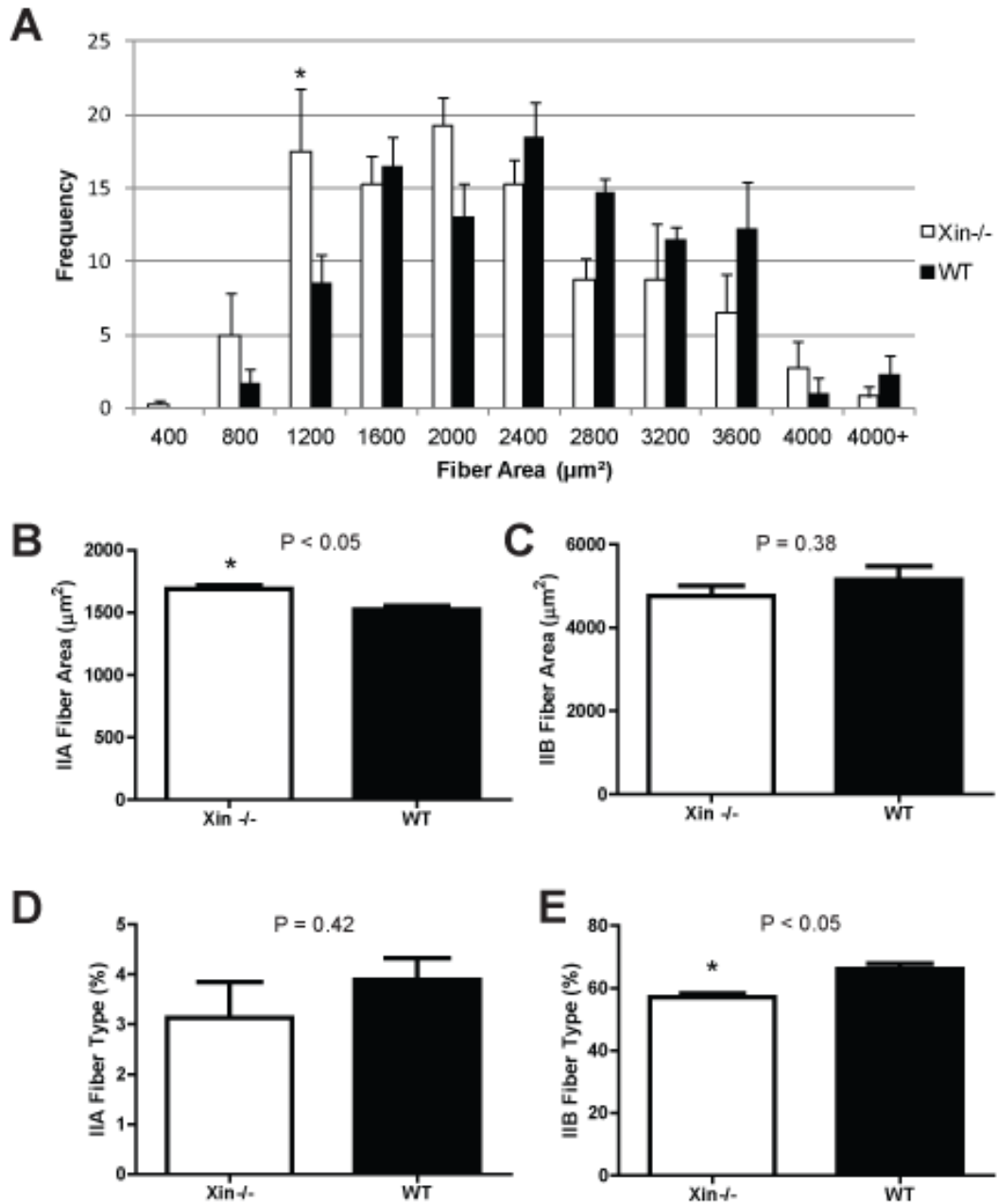


Figure 3.1: Xin^{-/-} TA muscle exhibits morphologic differences in fiber area and fiber type compared to WT. A: Muscle fiber areas were grouped by increasing size and the frequency of fibers in each group was determined. The histogram shows there is a trend

towards more small fibers in Xin^{-/-} muscle compared to WT, with a significant difference between 1200 and 1600 μm^2 (denoted by *). B and C: Type IIA and IIB fiber areas were measured, and mean area of Xin^{-/-} and WT fibers shown. There is a significant increase in Xin^{-/-} type IIA fiber area, but no difference in type IIB fiber size between the two groups. D and E: The number of type IIA and IIB fibers were calculated as a percent of total number of muscle fibers in a cross-section. There is no difference in IIA fiber type percent, however there is a significant decrease in the number of type IIB fibers in Xin^{-/-} mice compared to WT.

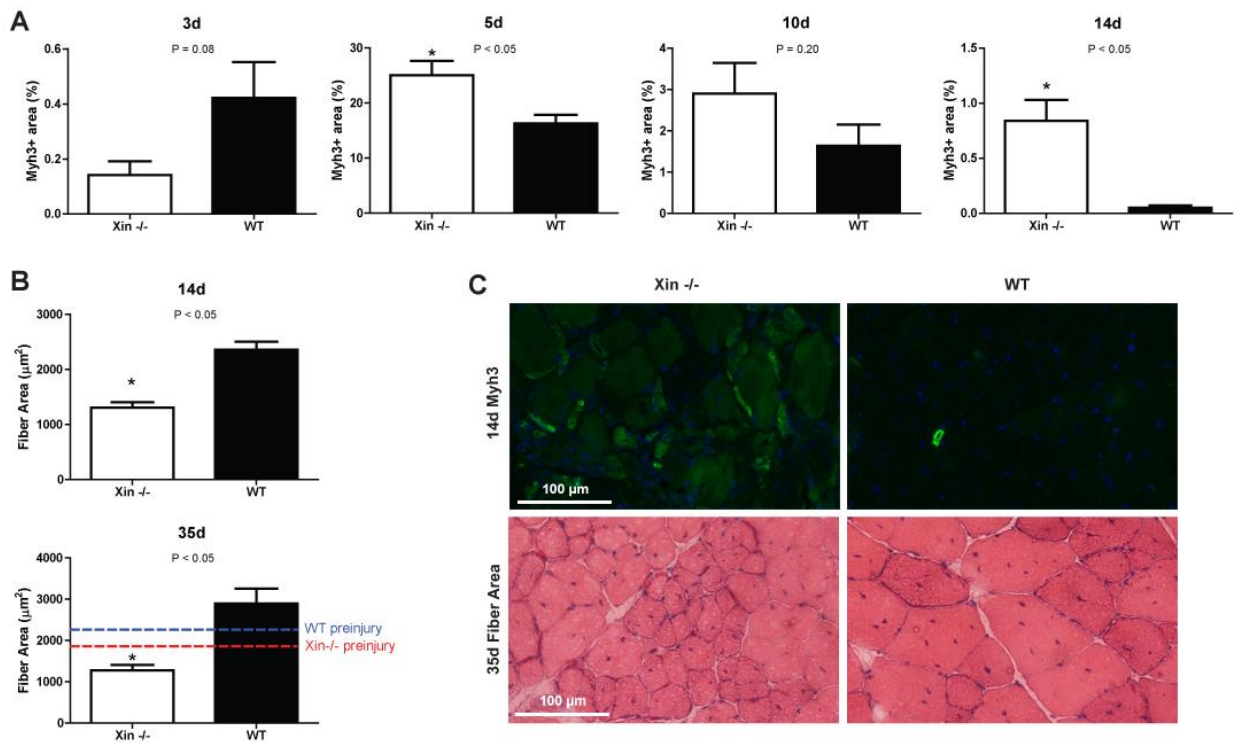


Figure 3.2: Skeletal muscle regeneration following cardiotoxin injury is impaired in Xin^{-/-} mice. A: The expression of embryonic myosin heavy chain (Myh3) as a percent of the total injured area was measured in Xin^{-/-} and WT TA muscle cross-sections, 3, 5, 10 and 14 days (d) post-injury. After 3 days of muscle repair, there is a trend towards less Myh3 in Xin^{-/-} muscle, suggesting a delay in the formation of new fibers. By 5 days of regeneration, there is significantly (*) more Myh3 in Xin^{-/-} muscle compared to WT, likely because expression in WT fibers has switched to mature myosin heavy chain. This trend continues after 10 and 14 days of regeneration. After 14 days of muscle repair, there is significantly (*) more Myh3 expression Xin^{-/-} fibers, where expression is almost non-existent throughout WT muscle. B: Muscle regenerative capacity of Xin^{-/-} and WT mice was also determined by analyzing TA muscle fiber cross-sectional area, 14 and 35 days after cardiotoxin injury. Xin^{-/-} fibers are significantly (*) smaller than WT after 14 days of muscle repair. After 35 days, WT fibers have exceeded pre-injury size (blue dotted line), whereas Xin^{-/-} fiber size is significantly (*) smaller and have not attained pre-injury size (red dotted line). C: Immunofluorescent and histochemical (H&E) stains of Xin^{-/-} and WT TA muscle cross-sections 14 and 35 days post-injury respectively. Immunofluorescent stain of Myh3 (bright green) in Xin^{-/-} TA muscle displays many small, immature Myh3-positive fibers, whereas WT muscle has mostly Myh3-negative fibers. The background staining was increased to display the association of Myh3-positive areas with the surrounding muscle. The H&E stain shows that Xin^{-/-} regenerating fibers, depicted with centrally located nuclei, are smaller than WT fibers, after 35 days of muscle repair.

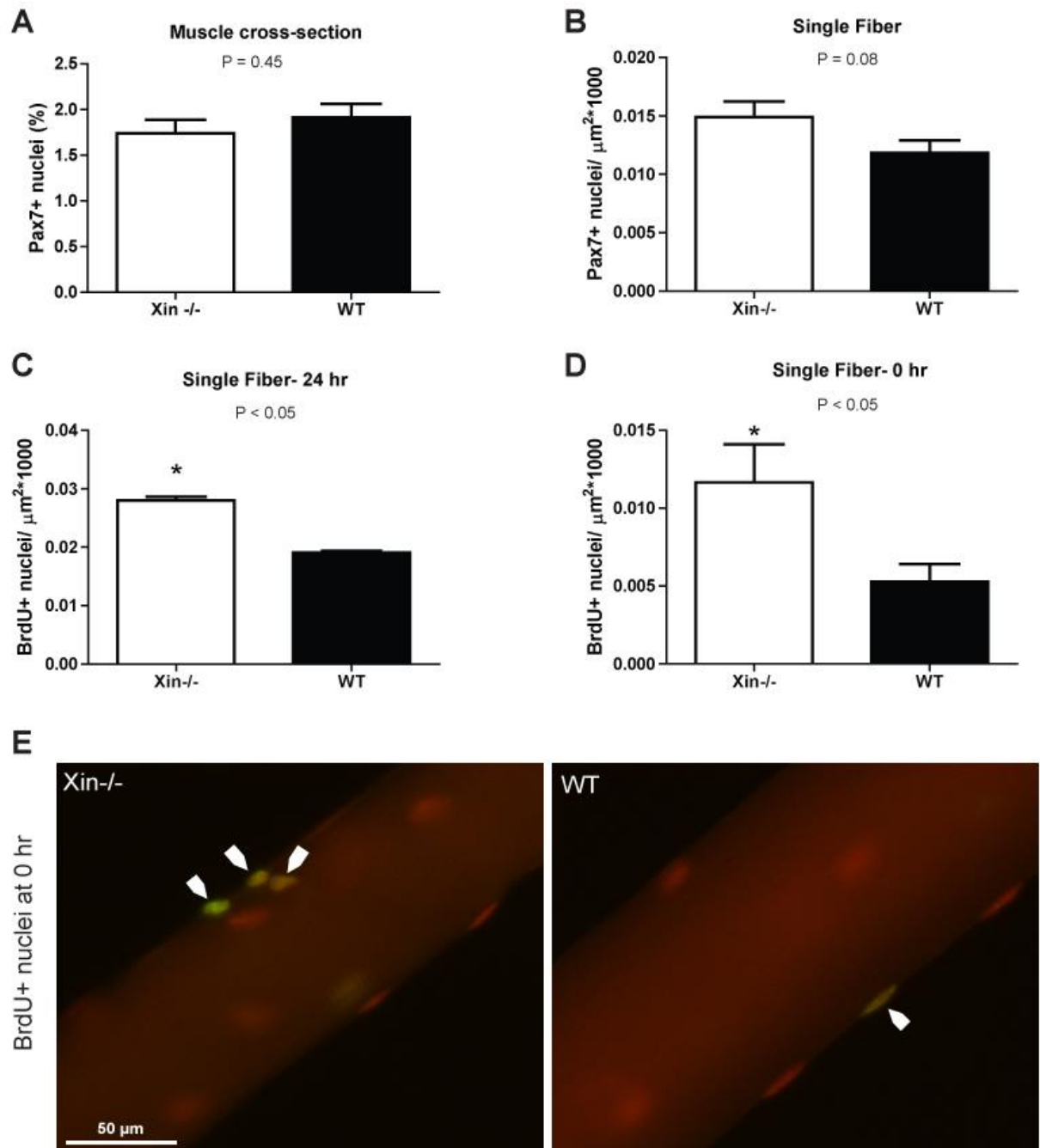


Figure 3.3: Xin^{-/-} satellite cells are hyperactivated compared to WT. A and B: The number of satellite cells in Xin^{-/-} and WT resting (uninjured) muscle was determined by analyzing Pax7 in TA muscle cross-section (A) and isolated myofibers from EDL and peroneus longus muscles (B). Pax7 positive SCs in muscle cross-section were determined as being co-localized with nuclei labelled with DAPI, and expressed as a

percentage of the total number of nuclei. In isolated single fibers, Pax7-positive SCs were expressed per μm^2 , which was calculated based on fiber surface area. In both analyses, there was no significant difference in the number of SCs at rest between Xin^{-/-} and WT muscle, however a slight increase in the number of Pax7⁺ SCs on Xin^{-/-} myofibers. C: BrdU is incorporated into activated satellite cells and was therefore used to determine the number of Xin^{-/-} and WT activated SCs associated with myofibers (per μm^2). There are significantly (*) more activated SCs on Xin^{-/-} single fibers compared to WT after 24 hours of in vitro incubation in BrdU. D: To determine if there are more activated SCs in Xin^{-/-} muscle at rest (0 hr) compared to WT, BrdU was injected into both animal groups and allowed to incorporate for 20 hours, before isolating single fibers. Results indicate a significant (*) increase in the number of activated SCs on Xin^{-/-} myofibers (per μm^2) compared to WT. E: BrdU-positive (arrow; green) nucleus on the myofiber periphery, with all nuclei labelled with propidium iodide (red). In the resting muscle (0 hr) Xin^{-/-} satellite cells are hyperactivated, since there are very few, if any, activated SCs in WT muscle.

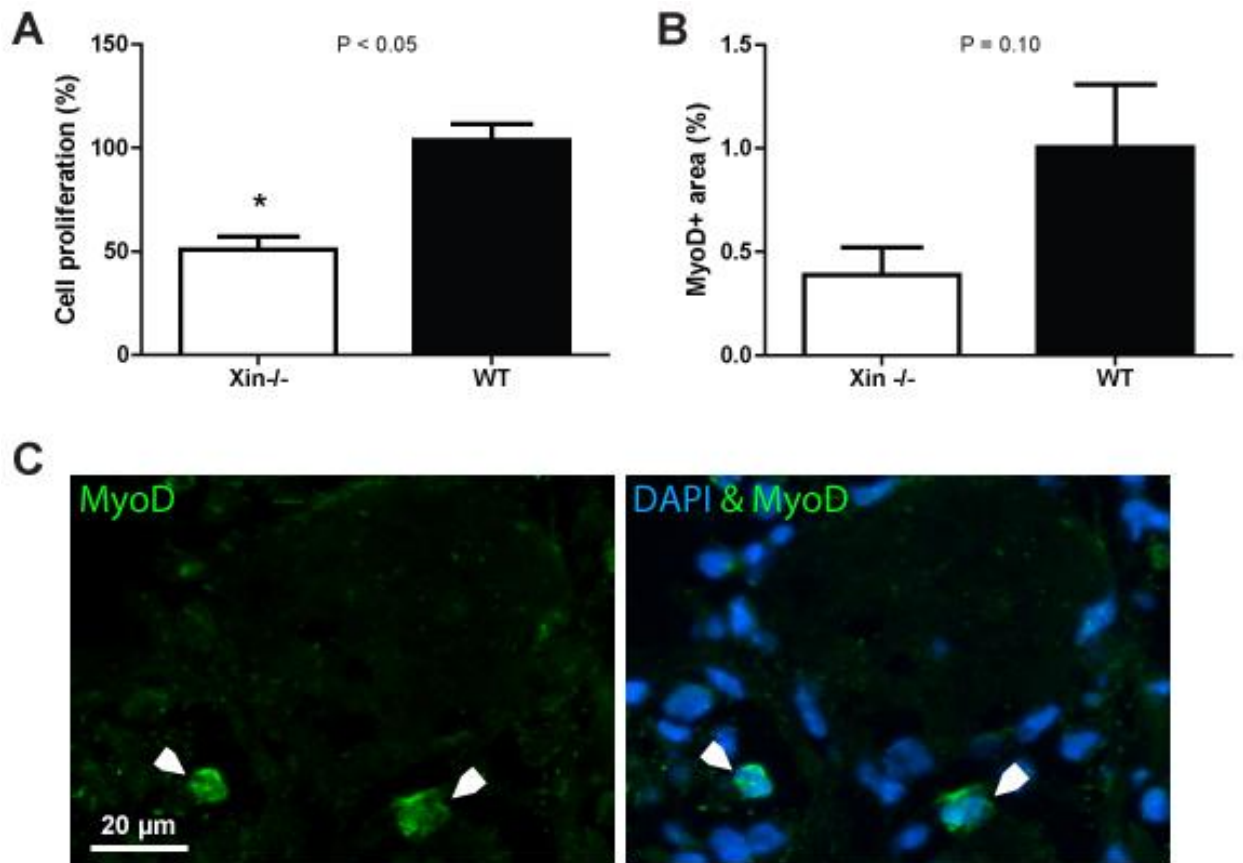


Figure 3.4: Satellite cell/myoblast proliferative capacity is reduced in Xin^{-/-} mice. A: Primary myoblasts were isolated from Xin^{-/-} and WT skeletal muscle, and the percent increase from the initial number of myoblasts was determined after 18 hours. Results indicate a significant (*) decrease in Xin^{-/-} myoblast proliferation compared to WT. B: MyoD is expressed in proliferating myoblasts early in the regenerative process. Xin^{-/-} and WT TA muscle sections were stained for MyoD 3 days post-injury, where there was a reduction, although not significant, in MyoD-positive area as a percent of total injured area, compared to WT. C: Immunofluorescent stain of MyoD-positive myoblasts (arrow; green), confirmed by co-localization with nuclei marker, DAPI (arrow; blue).

References

1. **Barash IA, Mathew L, Ryan AF, Chen J and Lieber RL.** Rapid muscle-specific gene expression changes after a single bout of eccentric contractions in the mouse. *Am J Physiol Cell Physiol* 286: 2: C355-64, 2004.
2. **Beatham J, Gehmlich K, van der Ven PF, Sarparanta J, Williams D, Underhill P, Geier C, Furst DO, Udd B and Blanco G.** Constitutive upregulations of titin-based signalling proteins in KY deficient muscles. *Neuromuscul Disord* 16: 7: 437-445, 2006.
3. **Bischoff R.** Cell cycle commitment of rat muscle satellite cells. *J Cell Biol* 111: 1: 201-207, 1990.
4. **Charge SB and Rudnicki MA.** Cellular and molecular regulation of muscle regeneration *Physiol Rev* 84: 1: 209-238, 2004.
5. **Cherepanova O, Orlova A, Galkin VE, van der Ven PF, Furst DO, Jin JP and Egelman EH.** Xin-repeats and nebulin-like repeats bind to F-actin in a similar manner. *J Mol Biol* 356: 3: 714-723, 2006.
6. **Crawford GL and Horowitz R.** Scaffolds and chaperones in myofibril assembly: putting the striations in striated muscle. *Biophys Rev* 3: 1: 25-32, 2011.
7. **Hawke TJ, Atkinson DJ, Kanatous SB, Van der Ven PF, Goetsch SC and Garry DJ.** Xin, an actin binding protein, is expressed within muscle satellite cells and newly regenerated skeletal muscle fibers. *Am J Physiol Cell Physiol* 293: 5: C1636-44, 2007.

8. **Hawke TJ and Garry DJ.** Myogenic satellite cells: physiology to molecular biology. *J Appl Physiol* 91: 2: 534-551, 2001.
9. **Hawke TJ, Jiang N and Garry DJ.** Absence of p21CIP rescues myogenic progenitor cell proliferative and regenerative capacity in Foxk1 null mice. *J Biol Chem* 278: 6: 4015-4020, 2003.
10. **Karalaki M, Fili S, Philippou A and Koutsilieris M.** Muscle regeneration: cellular and molecular events. *In Vivo* 23: 5: 779-796, 2009.
11. **Krause MP, Riddell MC and Hawke TJ.** Effects of type 1 diabetes mellitus on skeletal muscle: clinical observations and physiological mechanisms. *Pediatr Diabetes* 12: 4 Pt 1: 345-364, 2011.
12. **Nissar AA, Zemanek B, Labatia R, Atkinson DJ, van der Ven PF, Furst DO and Hawke TJ.** Skeletal muscle regeneration is delayed by reduction in Xin expression: consequence of impaired satellite cell activation? *Am J Physiol Cell Physiol* 302: 1: C220-7, 2012.
13. **Otten J, van der Ven PF, Vakeel P, Eulitz S, Kirfel G, Brandau O, Boesl M, Schrickel JW, Linhart M, Hayess K, Naya FJ, Milting H, Meyer R and Furst DO.** Complete loss of murine Xin results in a mild cardiac phenotype with altered distribution of intercalated discs. *Cardiovasc Res* 85: 4: 739-750, 2010.

14. **Seale P, Sabourin LA, Girgis-Gabardo A, Mansouri A, Gruss P and Rudnicki MA.** Pax7 is required for the specification of myogenic satellite cells. *Cell* 102: 6: 777-786, 2000.

15. **Sinn HW, Balsamo J, Lilien J and Lin JJ.** Localization of the novel Xin protein to the adherens junction complex in cardiac and skeletal muscle during development. *Dev Dyn* 225: 1: 1-13, 2002.

16. **Wozniak AC, Kong J, Bock E, Pilipowicz O and Anderson JE.** Signaling satellite-cell activation in skeletal muscle: markers, models, stretch, and potential alternate pathways. *Muscle Nerve* 31: 3: 283-300, 2005.

Chapter 4: PREFACE

Significance to thesis

The goal of this study was to determine if the increase of Xin expression during muscle regeneration in the mouse translates to myopathic states in humans by identifying Xin expression in damaged human skeletal muscle. Previous studies have shown that Xin expression is negligible within the ‘belly’ of uninjured mouse skeletal muscle but is upregulated in response to muscle damage and is important in the muscle repair process. Therefore this study is novel as it identifies a marker of muscle damage that is only present within the muscle belly of injured and regenerating skeletal muscle; a finding with important clinical and research implications. Since myopathic muscles are constantly undergoing degeneration/regeneration, the first aim of this study was to determine if Xin expression is increased within myopathic human muscle, and more importantly, does expression correlate with the degree of muscle damage. Furthermore, Xin expression was also analyzed in human muscle damaged by eccentric exercise to determine if the protein is a useful marker of all causes of muscle damage. In order to illustrate the efficacy of Xin to be used as a clinical marker of muscle damage severity, other possible markers were analyzed for comparison. Therefore the second aim of this study was to determine the protein expression profile of other candidate markers of muscle damage: Xirp2, Filamin-C and Collagen. These results have the ability to alter the way clinicians and researchers identify muscle damage in patients, and ultimately specify treatments based on the degree of muscle damage observed.

Contribution of Authors

Mats Nilsson contributed to the design of the study, performed experiments to assess Xin expression, and performed image analysis.

Aliyah A. Nissar performed experiments to assess Xirp2, Filamin-C and Collagen expression, performed image analysis, determined the degree of skeletal muscle damage for each subject, wrote the initial draft of the manuscript and edited subsequent drafts.

Mark A. Tarnopolsky contributed to the design of the study, provided myopathic subject biopsies and subject diagnosis.

Gianni Parise provided eccentrically damaged and control subject biopsies.

Boleslav Lach assisted in sectioning muscle biopsies for analysis.

Dieter O. Fürst and Peter F.M. van der Ven contributed to the refining the initial draft.

Thomas J. Hawke designed the study, reviewed data files and edited the manuscript.

Xin: A marker of skeletal muscle damage severity in myopathic patients

Mats Nilsson ^{*1}, Aliyah A. Nissar ^{*2}, Mark A. Tarnopolsky¹, Gianni Parise³, Boleslav Lach², Dieter O. Fürst⁴, Peter F.M. van der Ven⁴, Thomas J Hawke²

¹Dept of Medicine and Pediatrics, ²Pathology and Molecular Medicine, and ³Kinesiology. McMaster University. Hamilton ON. Canada, L8N 3Z5.

⁴Institute for Cell Biology, University of Bonn, NRW, Germany.

*Authors contributed equally to manuscript content

Running title: Xin expression in myopathy

Keywords: muscle repair, dystrophy, cytoskeleton, satellite cells

Word count: 4298

Correspondence and request for materials should be addressed to:

Thomas J. Hawke, Ph.D.

Pathology & Molecular Medicine, McMaster University,

1200 Main St. W., Hamilton ON. Canada, L8N 3Z5.

Phone: 905-525-9140 ext 22372

Email: hawke@mcmaster.ca

Abstract

Xin is a striated muscle-specific protein, where expression is isolated to the myotendinous junction of uninjured skeletal muscle and intercalated discs of the heart. However, upon muscle damage, Xin expression is upregulated and protein expression is observed throughout skeletal muscle fibers. In this study, Xin protein expression was analyzed immunofluorescently in the skeletal muscle of 47 subjects with various forms of myopathy, including muscular dystrophy, inflammatory myopathy, mitochondrial myopathy, metabolic myopathy, neuromyopathy and endocrine myopathy. Results indicate Xin expression is positively and significantly correlated ($r^2=0.4259$; $P<0.0001$) with the severity of muscle damage, regardless of myopathy. Other measures of muscle damage also showed a correlation with severity, such as collagen ($r^2=0.3878$; $P=0.0132$), and Xirp2 ($r^2=0.5197$; $P=0.0005$), however only Xin displayed an absence of expression within the healthy muscle belly. Therefore, Xin could be considered a useful clinical marker of disease severity in the previously mentioned myopathies, since any detectable expression is indicative of muscle damage. Given the strong correlation of Xin with damage severity in myopathy patients, we investigated the expression of Xin within the skeletal muscle of healthy subjects that had been subjected to eccentric exercise. Consistent with our aforementioned results, Xin expression was increased 24 hours after eccentric exercise (but not before) and was observable within the muscle belly of damaged fibers and within the activated muscle stem (satellite) cells. Taken together, these data demonstrate that Xin is a useful clinical marker of muscle damage given the strong correlation between the degree of damage and Xin expression. What's more, the

absence of expression outside the MTJ makes its detection within the muscle belly of injured muscle easy and quantifiable.

Introduction

Xin is a striated muscle-specific protein whose expression in the adult is within the intercalated discs (ICD) of the heart and the myotendinous junctions (MTJ) of skeletal muscle (4, 21) with no detectable expression in the ‘belly’ of healthy, uninjured, adult skeletal muscle (9, 18). However, this expression pattern changes dramatically in response to muscle injury suggesting that Xin contributes significantly to the remodeling/repair process of skeletal muscle (9).

Xin is the protein encoded by the gene ‘Xin-repeat protein 1’ (Xirp1) (previously referred to as ‘Cardiomyopathy associated 1’ or Cmya1) and is a member of the Xin-repeats actin-binding protein family, along with ‘Xin-repeat protein 2’ (Xirp2) which shares similar amino acid repeats with Xin (17, 21). Xin’s characteristic structural motifs allow for a variety of potential protein binding partners. Xin displays the ability to bind and cross-link F-actin, making them extra-resistant to depolymerisation (16). Xin also possesses several highly-conserved proline-rich regions allowing for binding to proteins containing consensus EVH1 domains (21). MENA/VASP (EVH1 domain-containing proteins) co-localize with, and directly bind the amino-terminus of Xin, while Filamin C, a muscle specific myotilin- and sarcoglycan-interacting protein, interacts with the C-terminus of Xin (21).

In adult skeletal muscle, the predominant theory regarding Xin’s function suggests that it is a multi-adaptor protein, involved in F-actin organization and stabilization, specifically at sites that involve considerable mechanical strain (18, 21). The role of Xin within regenerating skeletal muscle, however, has yet to be fully characterized. Given the

expression pattern of Xin within regenerating mouse skeletal muscle (15) and its role as a multi-adaptor protein within the cytoskeleton, we hypothesized that Xin would serve as a useful biomarker of muscle damage and, more importantly, as an indices of the degree of cytoskeletal disarray within myopathic or damaged skeletal muscle.

In the present study, skeletal muscle biopsies from 47 patients with various forms of myopathy, including but not limited to, limb-girdle muscular dystrophy (LGMD), facioscapulohumeral muscular dystrophy (FSHMD), mitochondrial myopathy, and inflammatory myopathy, were acquired and analyzed for Xin, collagen, Filamin-C and Xirp2 expression. Results indicate Xin expression is positively and significantly correlated with degree of muscle damage, regardless of myopathy. Although collagen, Filamin-C and Xirp2 also display a distinct expression pattern in highly damaged muscle, our results indicate that Xin is the most sensitive and reliable marker for muscle damage throughout the spectrum of muscle damage severity. Unlike the other candidate proteins, Xin expression is not detectable in healthy muscle fibers outside of the MTJ, and therefore could be considered a useful tool in research or clinical studies to determine even slight muscle damage instead of pathological diagnostics. In support of this conclusion, Xin expression was also observed to be upregulated in the muscle belly and within muscle satellite cells of eccentrically damaged muscle of healthy individuals. Thus, Xin would be considered a useful marker of damaged muscle regardless of etiology, whose expression is strongly and positively correlated with damage severity.

Materials/ Methods

Patients

A total of 47 myopathic patient biopsies were analyzed for Xin expression (appendix 1), and a subset of these biopsies were used for further immunohistochemical staining. Skeletal muscle biopsies were taken from the vastus lateralis of subjects with diverse myopathic conditions using a 5-mm Bergström needle, as previously described (20). Control muscle biopsies were taken from healthy male individuals from 18-25 years of age. Biopsies were also taken from healthy patients 24 hours after 300 maximal eccentric contractions (14). Permission for the study was obtained from the research ethics board at Hamilton Health Sciences.

Histochemical and Immunofluorescent Analyses

Frozen muscle biopsies were cut into 6- μ m cross-sections and adhered to charged glass slides for histochemical and immunofluorescent staining. Sections from all 47 myopathic biopsies were analyzed for Xin expression to determine if a correlation exists between Xin and muscle damage. A subset of subjects that displayed a strong Xin-to-damage correlation were further analyzed for Collagen, Filamin-C and Xirp2 expression.

Picrosirius red

To stain for collagen content, sections were incubated for 1 hr in picrosirius red solution containing 0.1% Direct Red 80 (Sigma 365548) in a saturated aqueous solution of picric acid (Sigma p6744). Sections were then rinsed in acidified water (0.5% acetic acid in

dH₂O) twice. After which sections were dehydrated in three changes of 100% ethanol, one change of xylene and coverslipped using Permount mounting media (Fisher Scientific, Toronto ON).

Immunofluorescent staining

Xin, Filamin-C and Xirp2 expression were detected using immunofluorescent staining. Firstly, sections were dried, fixed in cold methanol and acetone, then incubated for 30 min in blocking solution (10% normal goat serum, 1.5% bovine serum albumin, 0.3% triton). Primary antibodies were applied as follows: Xin for 1hr at room temperature (1:5; (21)), Filamin-C at 4° overnight (1:1000; courtesy of van der Ven, P.F. and Furst, D.O.), and Xirp2 at 4° overnight (1:10; (5)). A biotin-streptavidin detection system was used as recommended (Vector Labs, California, USA). After incubation in the appropriate biotinylated secondary antibody, a tertiary streptavidin antibody conjugated to dylight Alexa 594 (1:250) was applied for 30 min at room temperature. Blocking solution was re-applied before co-staining the sections with laminin (Abcam; ab14055), diluted 1:250 and incubated 4° overnight. Laminin was detected using an anti-chick Alexa 488 antibody (1:250), after which 4,6-diamidino-2-phenylindole (DAPI; 1:10,000) was applied to the sections for 5 min to identify nuclei.

In eccentrically damaged muscle, Xin was co-stained with dystrophin (Abcam; 15277) diluted 1:250, or a custom made affinity-purified Rad polyclonal antibody (Genway; 1mg/ml) diluted 1:150 and incubated at 4°C overnight. Sections were then incubated in

anti-rabbit (1:250) or anti-chick (1:300) Alexa 488 antibody respectively, followed by DAPI.

Muscle Damage Scoring System

Patient biopsies were assessed using three histopathological categories of muscle damage to determine an overall numerical damage score to which protein expression could be correlated (Fig. 4.1). Muscle damage scores were assigned for each category (out of 4), allowing for a total score of 12 based on multiple 20x images taken of each muscle section, stained with laminin and DAPI. The first category was the degree of nuclei infiltration assessed using DAPI where with increasing damage severity, nuclei begin to aggregate at the periphery of myofibers (scored as 1-2), within the extra cellular matrix (scored as 2 or 3), and within myofibers (scored as 3 or 4) (Fig. 4.1). Laminin can be used to identify signs of myopathy as it is a component of myofiber basement membranes (3) and is upregulated in the extracellular matrix (ECM) during muscle repair (10, 13). Therefore, damage was assessed by the increase in dysregulation of laminin expression directly surrounding each myofiber (scored as 1 or 2) and increased density of laminin in the ECM (scored as 3 or 4). Lastly, as muscle damage becomes more severe, myofiber size and shape becomes more variable as seen in Figure 4.1 and Kley et al. (2007) (12). Therefore, damage scores are greater as a larger area of muscle section displays increased myofiber variability. Using this system, myopathic biopsies were compared to control (score = 0), and the most damaged muscle subsequently received scores closer to 12.

Image analysis

Images of the immunostained muscle sections were captured in high resolution using a Nikon 90i Eclipse microscope. Threshold detection on Nikon Elements software was utilized to determine the percentage of positively-stained area in the total muscle section, determined as signal above the negative control.

Statistical Analysis

Linear regression analysis (r^2) was used to determine if a significant relationship exists between the severity of damage and the expression of Xin, collagen, Filamin-C and Xirp2 within the muscle, using GraphPad Prism software. Linear regression was significantly non-zero if $P < 0.05$.

Results

Xin expression increases with increasing severity of muscle damage

Xin expression as a percent of total muscle cross-sectional area was determined in subjects with various forms of myopathy (Fig. 4.2A) or in healthy subjects following eccentric exercise (Fig. 4.4). The degree of muscle damage in each subject, as assessed by nuclei infiltration, laminar dysregulation and fiber morphology (Fig. 4.1), when correlated with Xin levels revealed a significant and positive relationship (Fig. 4.2A; $N=49$; $r^2=0.4259$; $P<0.0001$). Control muscle from non-myopathic patients showed baseline levels of Xin close to 0 (Fig. 4.2A; Fig. 4.3a). In muscle with a low degree of damage, expression of Xin was detected at the intracellular periphery of the myofibers (Fig. 4.3b). In some instances, Xin co-localized with nuclei underneath the basal lamina, which is consistent with the documented expression pattern of Xin within satellite cells (9, 15). As the degree of muscle damage increased, as noted by increases in nuclei around the fiber periphery and fiber size/shape variability, Xin expression also increased around the myofiber periphery (Fig. 4.3c). In severely damaged muscle, where laminin expression in the ECM is increased and macrophages infiltrate damaged myofibers, Xin is highly expressed at the fiber periphery as well as within degenerating fibers (Fig. 4.3d). In healthy muscle that has been eccentrically damaged, Xin is upregulated 24 hours following exercise in the sublaminar region, assessed with dystrophin and DAPI. This is indicative of the localization of Xin to the satellite cell (Fig. 4.4a). Furthermore, Xin was co-localized with Rad, a marker of activated satellite cells in eccentrically damaged

muscle (Fig. 4.4b). These results indicate that the protein expression of Xin can be used as a marker of muscle damage severity.

Muscle damage scores are validated using collagen content

Collagen expression is elevated in damaged muscle resultant, in part, from increased need for ECM remodelling and the associated inflammatory response (3), therefore it was reasonable to validate the muscle damage scoring system against collagen content. Using a picrosirius red stain on a subset of muscle cross-sections from the 47 patients, our findings are consistent with previous findings (6, 7, 10, 13) demonstrating a significant positive correlation between muscle damage scores and collagen content (Fig. 4.2B; N=15; $r^2=0.3878$; P=0.0132). In undamaged (healthy control) and 'low-score' damaged muscle, collagen is located within the lamina of the myofiber, stained in red (Fig. 4.3e-f). As muscle damage becomes more extensive, collagen is deposited in the extracellular space between damaged muscle fibers shown in Fig. 4.3g-h, thereby increasing the percentage of collagen content in the total cross-sectional area.

Filamin-C expression does not correlate with severity of muscle damage

Filamin-C is located in the myofibrillar Z-disc, and at the myotendinous junction of skeletal muscle where it binds to Xin (21). Immunofluorescent staining on muscle cross-sections was performed to determine if Filamin-C protein expression was correlated with the degree of damage in muscle. In control, and low to moderately damaged muscle, Filamin-C expression was widespread but of low intensity, and similar between patients when analyzed as a percentage of total cross-sectional area (Fig. 4.3i-k). Conversely, in

highly damaged muscle, Filamin-C was found to aggregate in areas specific to muscle damage. Therefore, expression was less widespread but higher in intensity (Fig. 4.3l). As a result of these findings, there is no significant correlation between Filamin-C expression with increasing muscle damage severity (Fig. 4.2C; N=17; $r^2=0.1515$; P=0.1225).

Xirp2 is negatively correlated with severity of muscle damage

Xirp2 consists of Xin-repeats which are capable of binding actin, and is localized to the Z-disc region in skeletal muscle (11). Our results indicate that Xirp2 expression is highest as a percentage of area in control muscle, where it is consistently expressed in differing degrees of intensity in each myofiber (Fig. 4.3m). As muscle damage increases, Xirp2 expression is less consistent throughout the cross-sectional area (Fig. 4.3n,o). In severely damaged muscle (highest scored), Xirp2 aggregates are formed, resulting in high intensity staining, but reduced area fraction (Fig. 4.3p). Therefore, Xirp2 expression as a percentage of total cross-sectional area decreases as muscle damage increases, resulting in a significant negative correlation (Fig. 4.2D; N=19; $r^2=0.5197$; P=0.0005).

Discussion

Skeletal Muscle Regeneration- Determining Severity of Muscle Damage

Skeletal muscle has the capacity to undergo a relatively rapid regenerative process in response to muscle damage that is characterized by two general phases: degeneration of disrupted myofibers and subsequent repair of damaged fibers and/or *de novo* synthesis of new myofibers. In myopathic muscle this process is ongoing, and therefore severity of muscle damage can be determined, as done in this study, by assessing the presence of factors associated with regeneration.

During the initial phase of muscle degeneration, myofiber integrity is compromised resulting in necrosis, which is evident by increased serum levels of creatine kinase- a typical clinical marker of muscle damage (2). The myofiber external lamina is made up of collagen IV, laminin and heparin sulfate proteoglycans (6). Therefore in this study, disruption of myofiber integrity was determined by the degree of laminin dysregulation (Fig. 4.1). Laminin expression was further utilized to examine myofiber size and shape variability, which is characteristic of myopathic muscle (12). The degenerative phase is also marked by an activation of mononucleated inflammatory and myogenic cells, which were stained with DAPI (Fig. 4.1). These cells include neutrophils and macrophages which remove cellular debris (2). This allows for remodelling of the extracellular matrix (ECM) and an increase of ECM protein deposition such as collagen I, III, V and fibronectin necessary for structural stability of the muscle (6, 7). Therefore, collagen content was used as an identifier of muscle damage, and used to validate the muscle

damage scoring system (Fig. 4.2B; Fig. 4.3e-h). A significant positive correlation exists between muscle damage scores and collagen content, indicating it is appropriate to determine myopathic muscle damage severity based on laminar dysregulation, fiber variability and nuclei infiltration.

After the degenerative process, muscle regeneration occurs where activated satellite cells proliferate, and differentiate to form new myofibers, or fuse to existing damaged fibers in attempt to repair them (10). Characteristic of these fibers are centrally located myonuclei, stained with DAPI in Figure 4.1, indicative of severely damaged muscle (2).

Xin is the most suitable candidate for a marker of muscle damage severity

In uninjured skeletal muscle, Xin expression is negligible, and localized to the MTJ (18). In this study, we analyzed Xin expression in the skeletal muscle of subjects with a wide array of myopathies: muscular dystrophies (LGMD2A, LGMD2B, LGMD2I, LGMD2G, FSHMD, myotonic dystrophy, congenital muscular dystrophy), inflammatory myopathy, mitochondrial myopathy, metabolic myopathy, neuromyopathy, and endocrine myopathy (Supplementary Fig. 4.1; Supplementary Table 4.1). The importance of these findings is that Xin is a marker of damage severity in a variety of myopathies, and there appeared to be no significant relationship between Xin expression and any one disease. Therefore, Xin may be used to determine degree of muscle damage in any of the fore-mentioned myopathies.

Results also indicate that Xin expression is upregulated even in damaged healthy muscle 24 hours after eccentric exercise (Fig. 4.4). In eccentrically damaged muscle, and slightly

damaged myopathic muscle, Xin expression is found at the periphery of the myofiber, co-localizing with SC markers (Fig. 4.4; Fig. 4.3b). In moderately damaged muscle Xin expression increases at the myofiber periphery, and co-localizes with DAPI, which is indicative of expression within SCs (Figure 4.3c). In severely damaged myopathic muscle, Xin is expressed within regenerating fibers (Figure 4.3d), consistent with the expression pattern observed in injured mouse skeletal muscle (15). Therefore, Xin expression as a percentage of total muscle area is positively correlated with the degree of muscle damage in myopathic patients, regardless of the type of myopathy exhibited (Figure 4.2A).

Other candidate proteins examined include collagen, Filamin-C and Xirp2. Collagen content is known to increase as ECM remodelling ensues during regeneration. However, collagen is consistently expressed throughout healthy skeletal muscle, and therefore its expression pattern is less capable of deciphering between healthy, low and moderate degrees of muscle damage compared to Xin. For the same reason, Filamin-C and Xirp2 are not good markers for the degree of muscle damage in myopathic patients, as they are expressed at the Z-disc of uninjured fibers. However, these Z-disc proteins demonstrate a specific expression pattern in highly damaged muscle, where they aggregate within and around the periphery of regenerating fibers much like Xin (Fig. 4.3).

The expression of Xin within damaged skeletal muscle suggests a possible alternative to increased serum proteins in response to muscle damage, such as creatine kinase, myoglobin and troponin. Muscle damage resulting in the disruption to the ECM, basal lamina and sarcolemma result in the release of intracellular proteins, including creatine

kinase and myoglobin, which are not necessarily specific to skeletal muscle damage (1, 8). Other limitations of these proteins are that creatine kinase levels have been shown to be variable in exercise-induced muscle damage with the same magnitude of injury, and myoglobin is rapidly removed from circulation therefore serum level accuracy is time dependent (19). Since these cytosolic proteins may not be a direct indicator of the amount of structural damage, the presence of structurally-bound proteins in the plasma, such as troponin have been utilized. Troponin is striated-muscle specific contractile protein located on thin filaments, with fast-twitch and slow-twitch skeletal muscle specific isoforms which can give insight into differential damage to each fiber type (1). However, the clinical advantage of Xin as a muscle damage marker is the ability to determine the overall degree of damage in various myopathies, since plasma protein levels of the aforementioned proteins may not necessarily increase linearly with disease severity. Xin is a unique marker of damage as the location of expression, either at the myofiber periphery or in aggregates within damaged fibers, is pathologically significant in determining disease severity. Taken together, Xin expression can not only be utilized to determine if muscle is damaged, but also the degree of damage in various myopathies.

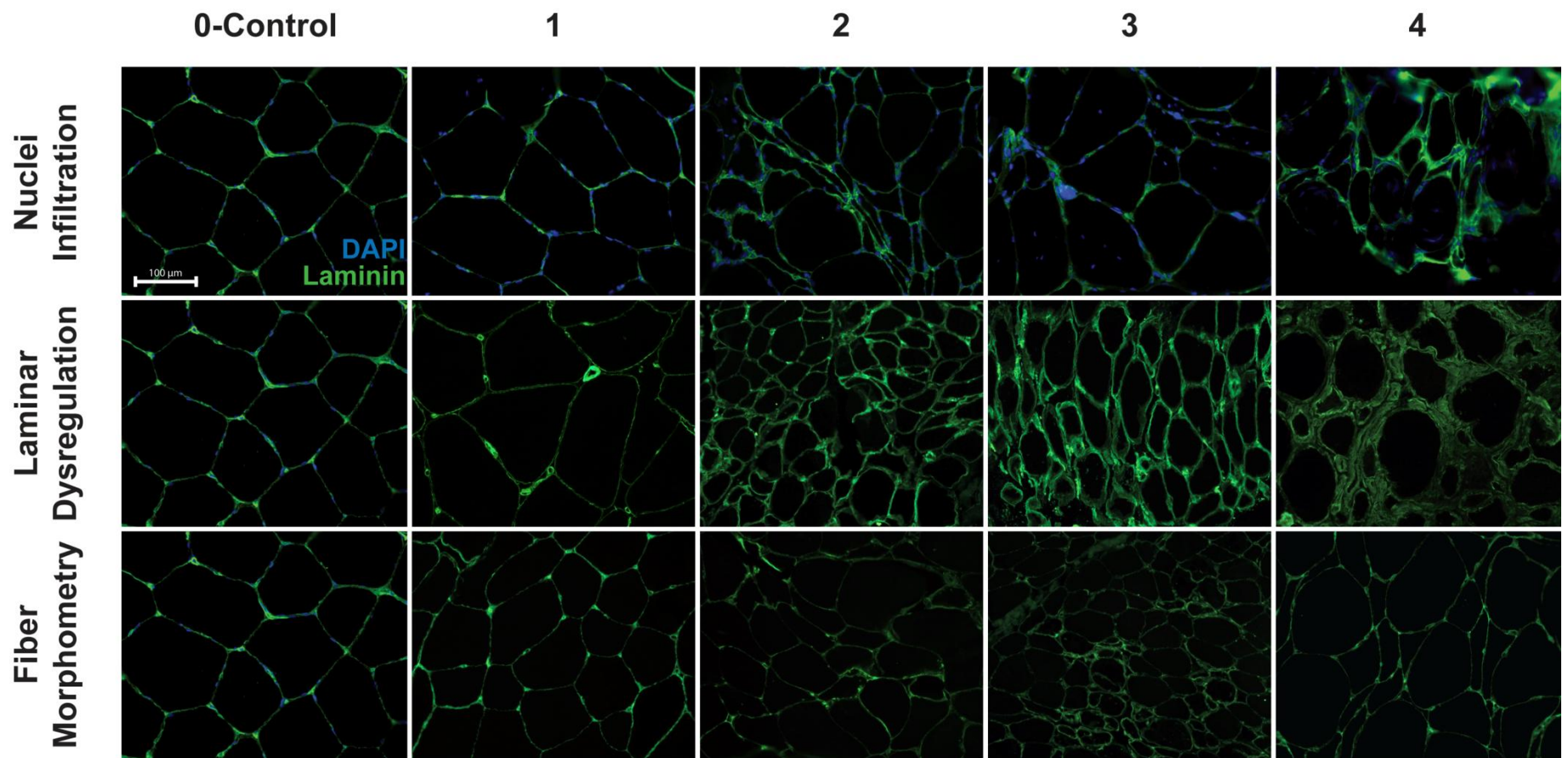


Figure 4.1: Muscle damage scoring system. The degree of skeletal muscle damage was assessed based on three histopathological indices: the degree of nuclei infiltration, laminar dysregulation, and the variability of myofiber shape/size. Myopathic muscle sections were stained for laminin (green) and nuclei marker DAPI (blue), and given a score out of 4 for each category, where 4 is the most severe dysregulation.

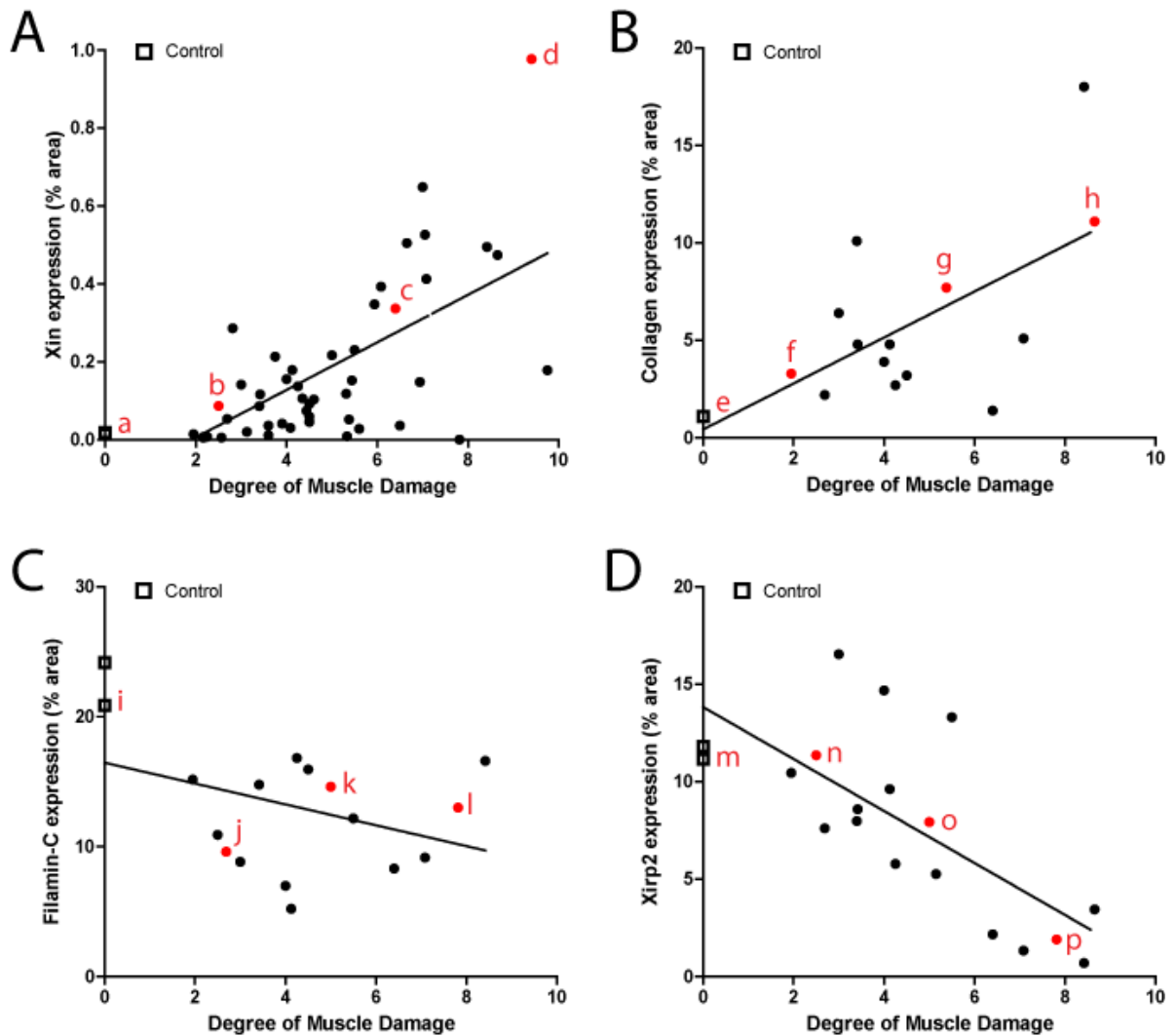


Figure 4.2: Correlation between proteins of interest and degree of muscle damage in myopathic patients. A: Xin expression as a percentage of total area in myopathic muscle is significantly and positively correlated with muscle damage severity. Xin expression of subjects *a* (control), *b*, *c*, and *d* are shown in Fig. 4.3. Xin expression in controls (*a*) is negligible. B: Collagen expression was also analyzed as a percent of total muscle-section area, and is significantly and positively correlated with degree of muscle damage. Representative images of subject *e* (control), *f*, *g*, and *h* are shown in Fig. 4.3. Collagen expression is evident in control samples. C: There is no significant relationship between Filamin-C expression and muscle damage severity. Images of subject *i* (control) to *l* is shown in Fig.4.3. Since Filamin-C is located in myofibrillar Z-discs, it is expressed in differing intensities in all myofibers in cross section, with only the highest intensity myofibers considered positive. Therefore control samples display the most uniform, thus highest expression of Filamin-C. D: Xirp2 expression in total muscle-section area is

significantly, but negatively correlated with degree of muscle damage. Expression in control subject (*m*), is consistent throughout the muscle section, which results in a high percentage expression in the total area. As the degree of muscle damage increases (subjects *n-p*; Fig. 4.3), Xirp2 aggregates to specific areas, therefore expression is less uniform throughout the entire muscle section.

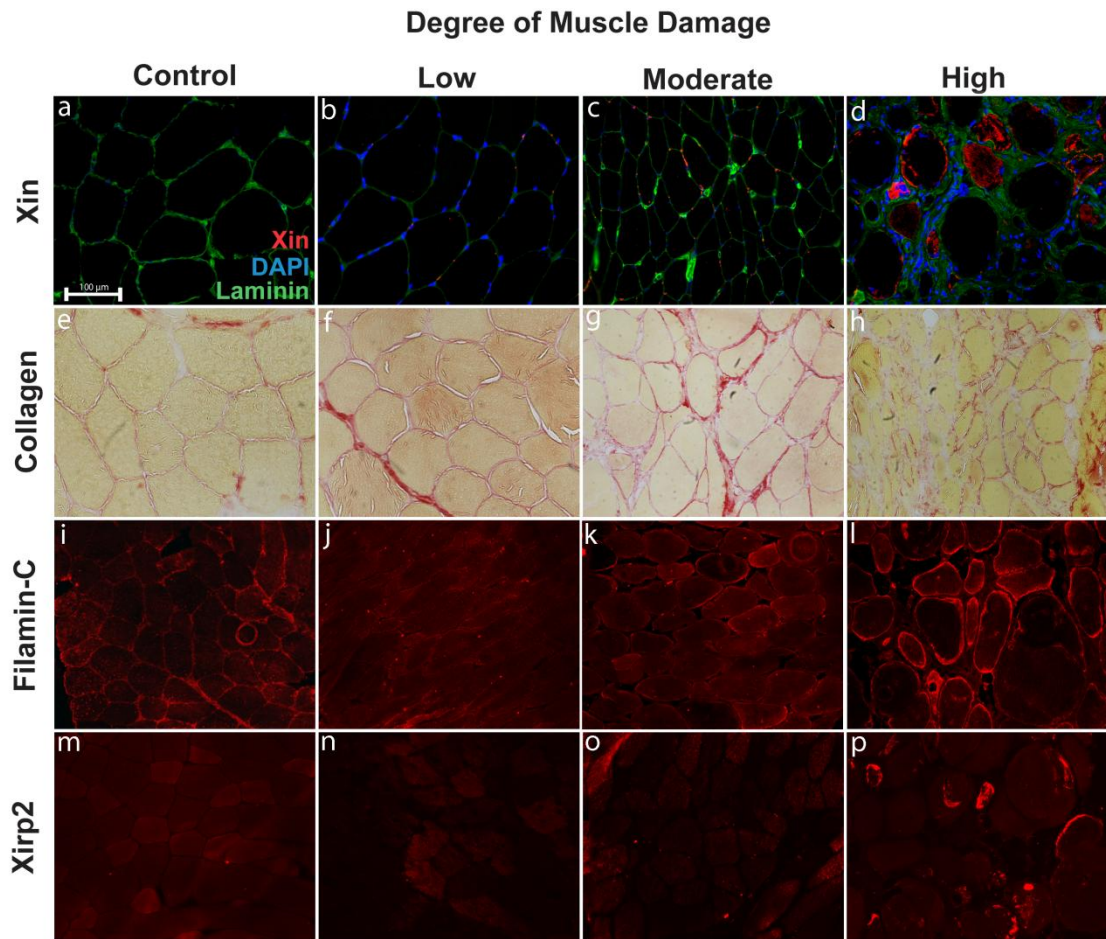


Figure 4.3: Xin, Collagen, Filamin-C and Xirp2 display differential expression patterns as muscle damage increases. Xin (*a-d*; red; Fig. 4.2A) expression is not detectable in control muscle, however expression increase and is displayed around the myofiber periphery in low and moderately damaged muscle. In highly diseased muscle, Xin expression is seen as aggregates within muscle fibers. Collagen (*e-h*; red; Fig. 4.2B) is found in the basal lamina of each muscle fiber in control subjects, and as damage increases and ECM remodelling ensues, collagen content increases. Filamin-C (*i-l*; red; Fig. 4.2C) is found in myofibrillar Z-discs and therefore expressed in differing degrees of intensity in myofibers in muscle cross-sections, where the fibers with the most intense expression were considered positive (Fig. 4.2C). In severely damaged muscle, intense

Filamin-C aggregation is noticed around and within some myofibers. Xirp2 (*m-p*; red; Fig. 4.2D) is also found in the muscle Z-disc and therefore is expressed in all myofibers with differing intensity in cross-sections in control subjects. As muscle damage increases, Xirp2 begins to aggregate and therefore expression of total cross-sectional area decreases, although expression is more intense within specific myofibers.

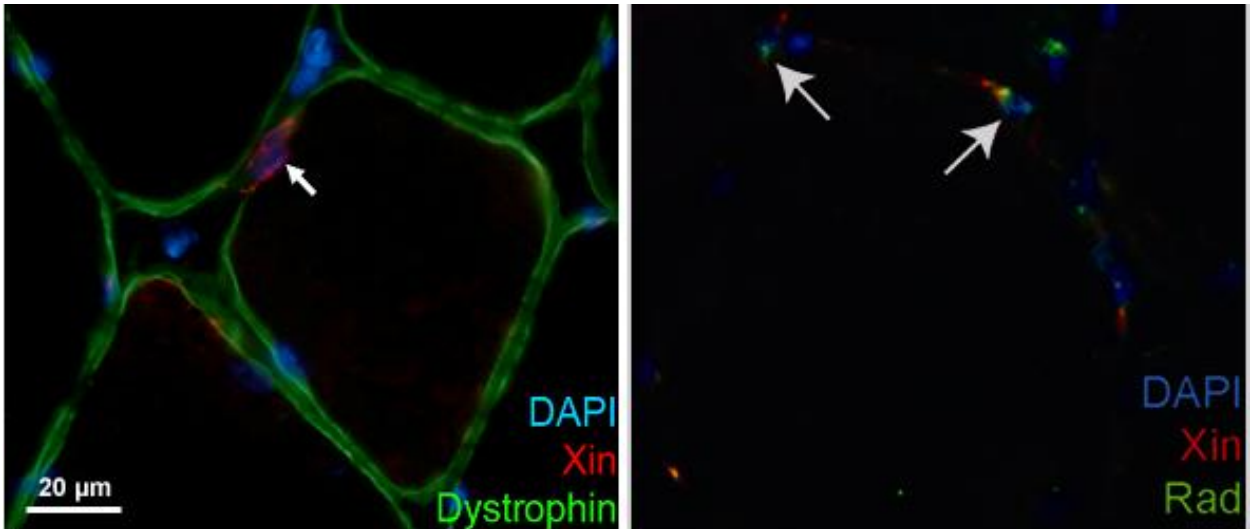
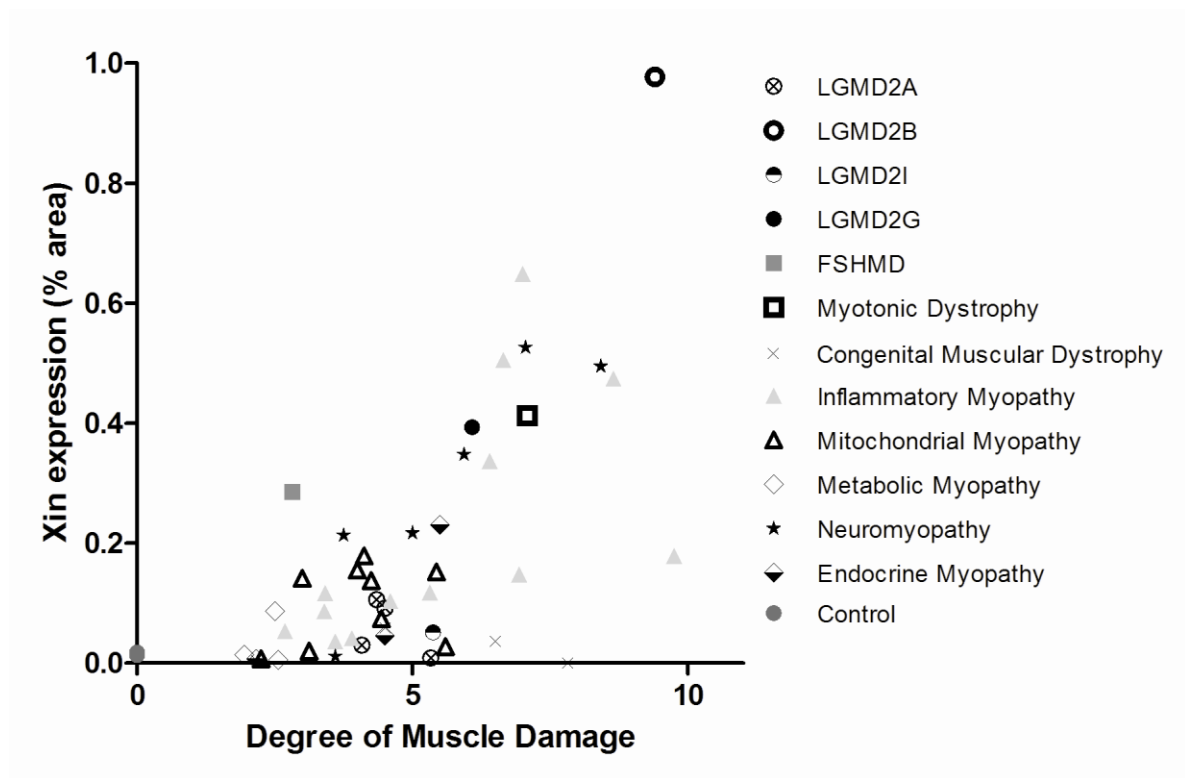


Figure 4.4: Xin expression in eccentrically damaged muscle from healthy subjects. Xin expression is increased 24 hours after exercise, and localized to muscle satellite cells. This is shown as Xin (red) is localized with activated satellite cell marker, Rad (green), and nuclei marker DAPI (blue), in the sublamellar region (assessed with dystrophin).

Acknowledgments:

The authors would like to thank the contributions of Bo Zhang for his excellent technical assistance. The authors would also like to thank the funding agencies that made this work possible: Canadian Institutes for Health Research [TJH].



Supplementary Figure 4.1: Xin expression in myopathic muscle grouped by disease. Xin expression is negligible in control muscle, however expression increases in various myopathies as muscle damage becomes more severe. There is no obvious relationship between any one myopathy and Xin expression, rather Xin expression is more prominent as muscle damage worsens in most disease states, and the highest expression is noticed in dysferlinopathy (LGMD2B).

Supplementary Table 4.1: Summary of subject profile. The Xin expression, muscle damage score and age of control subjects, and subjects with various forms of myopathy.

Patient ID	Damage Score	Xin Expression (%)	Age	Category
control	0	0.01811139	18-25	
control	0	0.0136261	18-25	
Disease 1	4.083333	0.03044128	?	LGMD2A
Disease 2	9.4	0.9773254	?	LGMD2B
Disease 3	5.333333	0.008646647	?	LGMD2A
Disease 4	4.5	0.09187317	?	LGMD2A
Disease 5	4.35	0.105896	?	LGMD2A
Disease 6	5.375	0.05163829	?	LGMD2I
Disease 7	6.083333	0.3931681	?	LGMD2G
Disease 8	6.4	0.3369129	?	Inflammatory myopathy
Disease 9	6.65	0.5048523	?	Inflammatory myopathy
Disease 10	3	0.1415405	47	Mitochondrial myopathy
Disease 11	2.8125	0.2860851	39	FSHMD
Disease 12	8.65	0.4741501	81	Inflammatory myopathy
Disease 13	7.05	0.5265492	41	Neuromyopathy
Disease 14	7.083333	0.4126863	74	Myotonic dystrophy
Disease 15	2.6875	0.05313873	38	Inflammatory myopathy
Disease 16	3.4	0.08602905	30	Inflammatory myopathy
Disease 17	3.6	0.03613281	76	Inflammatory myopathy
Disease 18	7	0.6486003	80	Inflammatory myopathy
Disease 19	2.5625	0.005378723	11	Metabolic myopathy
Disease 20	1.95	0.014328	19	Metabolic myopathy

Disease 21	2.166667	0.006993612	9	Endocrine myopathy
Disease 22	3.75	0.2131805	46	Neuromyopathy
Disease 23	5.5	0.2307129	55	Endocrine myopathy
Disease 24	3.416667	0.1166026	35	Inflammatory myopathy
Disease 25	5	0.2169609	43	Neuromyopathy
Disease 26	4.4375	0.07415771	36	Mitochondrial myopathy
Disease 27	5.4375	0.1521301	37	Mitochondrial myopathy
Disease 28	2.5	0.08657455	44	Metabolic myopathy
Disease 29	4	0.1553917	49	Mitochondrial myopathy
Disease 30	4.6	0.1035767	25	Inflammatory myopathy
Disease 31	2.166667	0.005162557	14	Congenital muscular dystrophy
Disease 32	4.25	0.13731	64	Mitochondrial myopathy
Disease 33	5.9375	0.3478241	61	Neuromyopathy
Disease 34	3.125	0.01998901	15	Mitochondrial myopathy
Disease 35	9.75	0.178566	?	Inflammatory myopathy
Disease 36	8.416667	0.4949951	?	Neuromyopathy
Disease 37	2.25	0.007451375	6	Mitochondrial myopathy
Disease 38	4.125	0.1788712	49	Mitochondrial myopathy
Disease 39	5.6	0.02770996	?	Mitochondrial myopathy
Disease 40	6.5	0.03634644	12	Congenital muscular dystrophy
Disease 41	6.9375	0.147934	?	Inflammatory myopathy
Disease 42	3.6	0.01141357	?	Neuromyopathy
Disease 43	4.5	0.04575093	?	Endocrine myopathy
Disease 44	4.5	0.05916595	?	Congenital muscular

				dystrophy
Disease 45	7.8125	0.000114441	?	Congenital muscular dystrophy
Disease 46	3.9	0.04147339	?	Inflammatory myopathy
Disease 47	5.3125	0.1179695	?	Inflammatory myopathy

References

1. **Chapman DW, Simpson JA, Iscoe S, Robins T and Nosaka K.** Changes in serum fast and slow skeletal troponin I concentration following maximal eccentric contractions. *J Sci Med Sport* 2012.
2. **Charge SB and Rudnicki MA.** Cellular and molecular regulation of muscle regeneration. *Physiol Rev* 84: 1: 209-238, 2004.
3. **Chen X and Li Y.** Role of matrix metalloproteinases in skeletal muscle: migration, differentiation, regeneration and fibrosis. *Cell Adh Migr* 3: 4: 337-341, 2009.
4. **Choi S, Gustafson-Wagner EA, Wang Q, Harlan SM, Sinn HW, Lin JL and Lin JJ.** The intercalated disk protein, mXinalpha, is capable of interacting with beta-catenin and bundling actin filaments [corrected]. *J Biol Chem* 282: 49: 36024-36036, 2007.
5. **Claeys KG, van der Ven PF, Behin A, Stojkovic T, Eymard B, Dubourg O, Laforet P, Faulkner G, Richard P, Vicart P, Romero NB, Stoltenburg G, Udd B, Fardeau M, Voit T and Furst DO.** Differential involvement of sarcomeric proteins in myofibrillar myopathies: a morphological and immunohistochemical study. *Acta Neuropathol* 117: 3: 293-307, 2009.
6. **Cornelison DD.** Context matters: in vivo and in vitro influences on muscle satellite cell activity. *J Cell Biochem* 105: 3: 663-669, 2008.

7. **Gillies AR and Lieber RL.** Structure and function of the skeletal muscle extracellular matrix. *Muscle Nerve* 44: 3: 318-331, 2011.
8. **Hawke TJ.** Muscle stem cells and exercise training. *Exerc Sport Sci Rev* 33: 2: 63-68, 2005.
9. **Hawke TJ, Atkinson DJ, Kanatous SB, Van der Ven PF, Goetsch SC and Garry DJ.** Xin, an actin binding protein, is expressed within muscle satellite cells and newly regenerated skeletal muscle fibers. *Am J Physiol Cell Physiol* 293: 5: C1636-44, 2007.
10. **Hawke TJ and Garry DJ.** Myogenic satellite cells: physiology to molecular biology. *J Appl Physiol* 91: 2: 534-551, 2001.
11. **Huang HT, Brand OM, Mathew M, Ignatiou C, Ewen EP, McCalmon SA and Naya FJ.** Myomaxin is a novel transcriptional target of MEF2A that encodes a Xin-related alpha-actinin-interacting protein. *J Biol Chem* 281: 51: 39370-39379, 2006.
12. **Kley RA, Hellenbroich Y, van der Ven PF, Furst DO, Huebner A, Bruchertseifer V, Peters SA, Heyer CM, Kirschner J, Schroder R, Fischer D, Muller K, Tolksdorf K, Eger K, Germing A, Brodherr T, Reum C, Walter MC, Lochmuller H, Ketelsen UP and Vorgerd M.** Clinical and morphological phenotype of the filamin myopathy: a study of 31 German patients. *Brain* 130: Pt 12: 3250-3264, 2007.

13. **Krause MP, Moradi J, Nissar AA, Riddell MC and Hawke TJ.** Inhibition of plasminogen activator inhibitor-1 restores skeletal muscle regeneration in untreated type 1 diabetic mice. *Diabetes* 60: 7: 1964-1972, 2011.
14. **McKay BR, Toth KG, Tarnopolsky MA and Parise G.** Satellite cell number and cell cycle kinetics in response to acute myotrauma in humans: immunohistochemistry versus flow cytometry. *J Physiol* 588: Pt 17: 3307-3320, 2010.
15. **Nissar AA, Zemanek B, Labatia R, Atkinson DJ, van der Ven PF, Furst DO and Hawke TJ.** Skeletal muscle regeneration is delayed by reduction in Xin expression: consequence of impaired satellite cell activation? *Am J Physiol Cell Physiol* 302: 1: C220-7, 2012.
16. **Pacholsky D, Vakeel P, Himmel M, Lowe T, Stradal T, Rottner K, Furst DO and van der Ven PF.** Xin repeats define a novel actin-binding motif. *J Cell Sci* 117: Pt 22: 5257-5268, 2004.
17. **Pacholsky D, Vakeel P, Himmel M, Lowe T, Stradal T, Rottner K, Furst DO and van der Ven PF.** Xin repeats define a novel actin-binding motif. *J Cell Sci* 117: Pt 22: 5257-5268, 2004.
18. **Sinn HW, Balsamo J, Lilien J and Lin JJ.** Localization of the novel Xin protein to the adherens junction complex in cardiac and skeletal muscle during development. *Dev Dyn* 225: 1: 1-13, 2002.

19. **Sorichter S, Mair J, Koller A, Gebert W, Rama D, Calzolari C, Artner-Dworzak E and Puschendorf B.** Skeletal troponin I as a marker of exercise-induced muscle damage. *J Appl Physiol* 83: 4: 1076-1082, 1997.

20. **Tarnopolsky MA, Pearce E, Smith K and Lach B.** Suction-modified Bergstrom muscle biopsy technique: experience with 13,500 procedures. *Muscle Nerve* 43: 5: 717-725, 2011.

21. **van der Ven PF, Ehler E, Vakeel P, Eulitz S, Schenk JA, Milting H, Micheel B and Furst DO.** Unusual splicing events result in distinct Xin isoforms that associate differentially with filamin c and Mena/VASP. *Exp Cell Res* 312: 11: 2154-2167, 2006.

Chapter 5: General discussion & Conclusion

Significance of the studies

Healthy adult skeletal muscle is a relatively stable tissue, which has the ability to undergo extensive repair and remodelling in response to physiological and pathological stressors, such as exercise-induced injury, or devastating myopathic conditions like Muscular Dystrophy. The capacity for muscle repair is largely attributed to satellite cells; the resident stem cell of skeletal muscle which become activated in response to muscle damage (6). Upon activation, satellite cells undergo significant growth and cytoskeletal remodelling before proliferating to create progeny termed myoblasts. Myoblasts have the ability to migrate to the site of injury and repair the damaged muscle by either fusing to a damaged myofiber, or forming new myofibers (6). Despite the fundamental role of satellite cells in the muscle repair process, basic mechanisms that govern their function are largely unknown, thus their therapeutic potential as a stem cell population is unfulfilled. The results of these studies have contributed to the understanding of satellite cell function, as the protein Xin which was previously found as being upregulated in response to muscle damage (5), was identified as being localized with satellite cell specific markers, important in satellite cell activation, and overall regeneration in mouse skeletal muscle. Xin expression in murine muscle repair also translates to human myopathic muscle, where expression is increased as the degree of muscle damage increases. This finding is clinically relevant, as Xin can be used as a marker to determine minimal to advanced muscle damage regardless of presenting myopathy, useful in streamlining therapies based on disease severity.

Overall findings and future directions

Two experimental models were utilized to determine alterations within skeletal muscle satellite cells, and the muscle repair process when Xin expression is reduced: adenoviral-mediated Xin shRNA, and a Xin-deficient mouse model. Both of these models presented advantages and limitations. Mainly, the administration of Xin shRNA in wild-type muscle would diminish the contribution of alternate proteins which may compensate for the reduction of Xin during development, however this method only resulted in a ~60% reduction of endogenous Xin (5, 8). Whereas the Xin^{-/-} mouse model is completely deficient of all Xin isoforms, however it is likely compensatory proteins arose during development, since Xin^{-/-} display no overt phenotype (9). Importantly, both models demonstrate impaired skeletal muscle regeneration, even after 14 and 35 days post-injury, assessed by Myh3 expression and reduced Xin^{-/-} myofiber size. Results suggest impaired regeneration may be due to altered satellite cell activation when Xin is hypothesized to be involved in cytoskeletal remodeling, as satellite cell activation is reduced in the Xin shRNA model and hyperactivated in Xin-deficient mice. It is also hypothesized that compensatory proteins present in Xin^{-/-} mice promote satellite cell hyperactivation, however are detrimental to satellite cell proliferation, since no affect on proliferation is observed in the Xin shRNA model. This hypothesis can be tested by identifying the expression of another protein in the Xin-repeat family, Xirp2 (10). Other possibilities for compensatory proteins are nebulin-repeat proteins such as N-RAP, which bind to f-actin similarly to Xin-repeat proteins, and is involved in myofibril assembly (1, 3, 4). Admittedly, these studies do not examine satellite cell chemotaxis and differentiation,

which would be useful to bridge the disconnect between proliferative capacity and overall muscle regeneration. Also, even though it is hypothesized that Xin plays a role in cytoskeletal remodelling, to elucidate the exact function of Xin during satellite cell activation, future studies should aim to determine novel Xin binding partners within the satellite cell.

These studies also suggest that Xin plays a dual role in the skeletal muscle regeneration process: specifically within the satellite cell and also within regenerating fibers. Xin expression is observed in regenerating mouse muscle 5 days post-injury, a time point where myofiber growth is occurring, lending to the hypothesis that Xin is involved in myofibrillar assembly. This translates to human myopathic muscle which undergoes constant degeneration and regeneration, where Xin expression is upregulated and found in aggregates within fibers. The accumulation of Xin within muscle fibers is also observed in filaminopathy subjects, which is caused by a mutation in the Filamin-C gene and results in focal myofibrillar destruction (7). Given that Xin is expressed at the MTJ in resting muscle (11), a location of high-mechanical stress, it is possible that Xin acts as structural support within highly degenerated muscle fibers.

Future directions should also aim to characterize Xin in myopathic patients of unknown etiology, since mutations in cytoskeletal proteins are known to lead to myopathic conditions (limb-girdle muscular dystrophy, myofibrillar myopathy, filaminopathy) (2, 7), mutations of Xirp1 may result in a novel form of myopathy, 'Xinopathy'. Since many patients are diagnosed with muscular dystrophy with unknown molecular defect, a

definitive diagnosis will assist in providing appropriate therapeutic strategies, thereby improving quality of life.

References

1. **Cherepanova O, Orlova A, Galkin VE, van der Ven PF, Furst DO, Jin JP and Egelman EH.** Xin-repeats and nebulin-like repeats bind to F-actin in a similar manner. *J Mol Biol* 356: 3: 714-723, 2006.
2. **Claeys KG, van der Ven PF, Behin A, Stojkovic T, Eymard B, Dubourg O, Laforet P, Faulkner G, Richard P, Vicart P, Romero NB, Stoltenburg G, Udd B, Fardeau M, Voit T and Furst DO.** Differential involvement of sarcomeric proteins in myofibrillar myopathies: a morphological and immunohistochemical study. *Acta Neuropathol* 117: 3: 293-307, 2009.
3. **Crawford GL and Horowitz R.** Scaffolds and chaperones in myofibril assembly: putting the striations in striated muscle. *Biophys Rev* 3: 1: 25-32, 2011.
4. **Gehmlich K, Geier C, Osterziel KJ, Van der Ven PF and Furst DO.** Decreased interactions of mutant muscle LIM protein (MLP) with N-RAP and alpha-actinin and their implication for hypertrophic cardiomyopathy. *Cell Tissue Res* 317: 2: 129-136, 2004.
5. **Hawke TJ, Atkinson DJ, Kanatous SB, Van der Ven PF, Goetsch SC and Garry DJ.** Xin, an actin binding protein, is expressed within muscle satellite cells and newly regenerated skeletal muscle fibers. *Am J Physiol Cell Physiol* 293: 5: C1636-44, 2007.
6. **Hawke TJ and Garry DJ.** Myogenic satellite cells: physiology to molecular biology. *J Appl Physiol* 91: 2: 534-551, 2001.

7. **Kley RA, Hellenbroich Y, van der Ven PF, Furst DO, Huebner A, Bruchertseifer V, Peters SA, Heyer CM, Kirschner J, Schroder R, Fischer D, Muller K, Tolksdorf K, Eger K, Germing A, Brodherr T, Reum C, Walter MC, Lochmuller H, Ketelsen UP and Vorgerd M.** Clinical and morphological phenotype of the filamin myopathy: a study of 31 German patients. *Brain* 130: Pt 12: 3250-3264, 2007.

8. **Nissar AA, Zemanek B, Labatia R, Atkinson DJ, van der Ven PF, Furst DO and Hawke TJ.** Skeletal muscle regeneration is delayed by reduction in Xin expression: consequence of impaired satellite cell activation? *Am J Physiol Cell Physiol* 302: 1: C220-7, 2012.

9. **Otten J, van der Ven PF, Vakeel P, Eulitz S, Kirfel G, Brandau O, Boesl M, Schrickel JW, Linhart M, Hayess K, Naya FJ, Milting H, Meyer R and Furst DO.** Complete loss of murine Xin results in a mild cardiac phenotype with altered distribution of intercalated discs. *Cardiovasc Res* 85: 4: 739-750, 2010.

10. **Pacholsky D, Vakeel P, Himmel M, Lowe T, Stradal T, Rottner K, Furst DO and van der Ven PF.** Xin repeats define a novel actin-binding motif. *J Cell Sci* 117: Pt 22: 5257-5268, 2004.

11. **van der Ven PF, Ehler E, Vakeel P, Eulitz S, Schenk JA, Milting H, Micheel B and Furst DO.** Unusual splicing events result in distinct Xin isoforms that associate differentially with filamin c and Mena/VASP. *Exp Cell Res* 312: 11: 2154-2167, 2006.